THESIS

THE ROLE OF PRION PROTEIN GLYCOSYLATION IN PRION PROPAGATION

Submitted by

Deandra Leigh Walker

Department of Microbiology, Immunology, and Pathology

In partial fulfillment of the requirements

For the Degree of Master of Science

Colorado State University

Fort Collins, Colorado

Spring 2018

Master's Committee:

Advisor: Glenn Telling

James Bamburg
Brendan Podell
Mark Zabel

ABSTRACT

THE ROLE OF PRION PROTEIN GLYCOSYLATION IN PRION PROPAGATION

Transmissible Spongiform Encephalopathies (TSEs) are a group of neurodegenerative diseases that affect humans and animals alike. TSEs are caused by the accumulation of a disease producing isoform referred to as PrP^{Sc} that results from the misfolding of the normal cellular prion protein PrP^{C}. The pathological outcomes of TSEs include amyloid plaque build-up and spongiform degeneration in the brain of infected hosts. Clinical signs of prion disease can vary between TSEs, but often include neurologic impairment that is subtle in onset and tends to progress slowly. Prion diseases are relatively recently discovered and have sparked much controversy due to the scientific findings that directly challenge some of the most well established scientific dogmas. Among these is that the infectious agent responsible for the transmission of TSEs is proteinacious in nature and devoid of the nucleic acids present in pathogens like viruses and bacteria. As a result of this hypothesis, both PrP^{C} and PrP^{Sc} share the same amino acid sequence in the host. Therefore, central to our understanding of the prion hypothesis is to recognize the structural differences between PrP^{C} and PrP^{Sc}. PrP^{C} has been proven to include three α-helices and two, short β-pleated sheets whereas PrP^{Sc} consists of high β-sheet content, aggregates in the presence of detergents, and is resistant to protease treatment. These characteristics of PrP^{Sc} have inhibited researchers to successfully examine the abnormal isoform in high-resolution structural studies. Therefore, an alternative means of distinguishing PrP^{C} and PrP^{Sc} is necessary.

Since then, several groups have created monoclonal antibodies (mAbs) that differentiate between infectious prion protein (PrP) aggregates. Two such mAbs, PRC5 and PRC7 were the first mAbs discovered in which the involvement of individual residues in functional, discontinuous, and conformationaly dependent epitopes was studied. Of these antibodies, PRC7, is dependent on N-linked glycosylation at mono-1 of the prion protein and specifically binds to the infected isoform of PrP. Therefore, we hypothesized that an underglycosylated form of PrP is preferentially generated during prion replication in the infected host. In this body of work, we have systemically ablated mono-1, one of the two N-linked glycan attachment sites on the murine prion protein to address the role of underglycosylation in prion propagation at N180 and at S/T182 of the consensus sequence by mutating N or S/T to each of the other 19 amino acids individually. Here we present novel evidence showing the effects of underglycosylation in prion propagation of prion isolates RML, 22L, 139A, and mCWD. These preliminary data demonstrate the importance of post-translational differences between PrP^{C} and PrP^{Sc} which represent a fundamental, unresolved aspect of the prion hypothesis.

ACKNOWLEDGEMENTS

First and foremost, I would like to thank my family, especially my parents, for allowing me to realize my own potential and encouraging me to explore it whole-heartedly. The support you have provided along the way has been the greatest gift you could have given me.

Second, I would like to thank all of my friends, you know who you are. Thank you for sharing in my triumphs and helping me through the pitfalls life brings.

Third, I need to thank the members of the Telling lab, both old and new, who have helped me complete this project in one form or another, and who have created a welcoming environment in the lab; Dr. Hae-Eun Kang, Dr. Julie Moreno, Dr. Jifeng Bian, Dr. Sehun Kim, Dr. Lindsay Parrie, Dr. Sarah Kane, Jenna Crowell, and Vanessa Selwyn.

Next, I would like to thank my graduate committee. To my advisor, Dr. Glenn Telling, thank you for believing in me. To Drs. Mark Zabel, James Bamburg, and Brendan Podell, thank you for sharing your expertise and for your continued support.

Finally, I would like to thank Jeffrey Near. Without your unconditional love and encouragement at home, I do not know if I would have ever achieved this accomplishment. I love you.

DEDICATION

This body of work is dedicated to my unborn son, Liam LeRoy Near. I cannot wait to meet you!

TABLE OF CONTENTS

LIST OF TABLES

LIST OF FIGURES

CHAPTER 1 – INTRODUCTION

Prion Diseases

Introduction to Transmissible Spongiform Encephalopathies

Prion diseases encompass a variety of unique ailments that affect animals and humans alike. These diseases are collectively referred to as Transmissible Spongiform Encephalopathies. The hallmarks of TSEs include a combination of spongiform change, astrocytic inflammation, neuronal loss, as well as amyloid plaques that build up and cause impaired brain function that worsen overtime.

History of Animal TSEs

Scrapie is the prototypic prion species causing disease in both sheep and goats. Because scrapie has been recognized for over 200 years in Europe, it has often been referred as the main reference for prion diseases, especially as it has become a worldwide epidemic (McGowan and Scott, 1922).

More recently recognized animal prion diseases have been described in both captive and wild animals. These include transmissible mink encephalopathy (TME), feline spongiform encephalopathy (FSE), chronic wasting disease (CWD), and bovine spongiform encephalopathy (BSE). In all of these cases, infected animals exhibit some combination of clinical signs that are usually insidious in onset and tend to progress slowly. In these TSEs, signs tend to be neurologic in nature and once they appear, these diseases are relentlessly progressive and fatal.

TME has been described as a rare, sporadic TSE that affects ranch-raised mink that are bred for their pelts. The only constant factor in the spread of TME is mink feed. Clinical signs of this disease differ from other animal TSEs in that the mink initially become hyperactive and aggressive before exhibiting other clinical signs of prion disease (Hadlow, 1999; Harstough and Burger, 1965; Marsh et. al., 1991; Marsh and Hadlow, 1992; and McKenzie et. al., 1996**)**. FSE, a TSE of domestic and captive wild cats was originally identified in 1990 (Gruffydd-Jones et. al., 1992; Wyatt et. al., 1991). Naturally occurring CWD is a TSE of deer and elk highly prevalent in North America and parts of Canada and uniquely affects both free-ranging and captive cervid populations (Spraker et. al., 1997; Williams and Young, 1980). More recently, CWD has been detected in moose and reindeer in Europe (Benestad et. al., 2016). Finally, BSE, a TSE of cattle, rapidly developed into an endemic in the United Kingdom (UK) as a result of recycling contaminated feed in industry farms (Anderson et. al., 1996; Collinge, 2001; Hadlow, 1999; Wells et. al., 1987; Wilesmith et. al., 1988).

History of Human TSEs

Human prion diseases are classified into several groups that include Creutzfeldt-Jakob disease (CJD), Gerstmann-Straussler syndrome (GSS), and kuru. These human TSEs are organized further into three etiological categories: sporadic, acquired, and inherited (Collinge, 2001; Soto, 2007).

Acquired prion diseases include iatrogenic CJD and kuru, which arise through the contamination in medical procedures or by cannibalistic rituals (Alpers et. al., 1987).

Sporadic CJD is rapidly progressive disease that arises randomly and occurs all over the world. It also accounts for the majority of all recognized human prion diseases, occurring in a large percentage of all reported human cases (Palmer et. al., 1991). Lastly, inherited prion diseases like GSS, familial CJD, and fatal familial insomnia (FFI), are associated with coding mutations in the prion protein gene (Collinge, 1997).

There is also evidence of another segmentation of human prion disease called variant CJD (vCJD) in the UK. Experimental data shows that vCJD is cause by the same prion strain that causes BSE in cattle leading to the concern that dietary exposure to BSE prions may lead to an epidemic of vCJD in the human population in the UK (Collinge, 1999; Cousens et. al., 1997; Ghani et. al., 1998; Hill et. al., 1997).

Collectively, concerns of zoonotic potential combined with iatrogenic transmission have intensified efforts for investigators to better understand prion propagation at the molecular level. This is necessary to further develop new and effective therapeutic and preventative treatments for prion diseases.

Transmissibility

In 1936, scrapie was shown to be transmissible by inoculation into uninfected sheep and goats (Cuille and Chelle, 1936). In these studies, researchers observed extended incubation times to the onset of observable disease-like symptoms. Because of this result, it was initially thought that the causative agent was viral in nature. In 1954,

Sigurdsson coined the term slow-acting infection to represent the phenomenon (Sigurdsson, 1954).

Around that same time, there was growing interest in an epidemic occurring in the Fore linguistic group of Eastern Highlands of Papa New Guinea because of a neurodegenerative disease called kuru, the prominent clinical aspect being progression into ataxia. Eventually, several groups of researchers concluded that kuru was being transmitted during cannibalistic feasts. And in 1959, Hadlow brought attention to kuru by citing the remarkable similarities it shares with scrapie. He ultimately suggested that the two diseases were parallel in their epizootiological, etiological, clinical, and pathological features indicating that these diseases could also be transmissible (Hadlow, 1959).

The next major turning point in the field came in 1966 when Gajdusek successfully transmitted kuru into chimpanzees by inoculation into the brain. Gibbs also showed that the same transmission was true of CJD in 1968, and later Masters in 1981 with GSS (Gajdusek et. al., 1966; Gibbs et. al., 1968; Masters et. al., 1981). Collectively, these studies eventually led to the concept of “transmissible dementias” which encompasses a variety of neurodegenerative conditions (Collinge, 2001).

The Prion Protein

Protein Only Hypothesis

Unlike other infectious agents, the infective agent of prion disease has proven to be unusual and has been a part of debate for some time. In the past, investigators argued

that the infective agent was made of a nucleic acid genome because 1. the pathogen behaved like a virus and 2. “strains” or distinct isolates of the pathogen exhibited different biological properties such as incubation times and patterns of spongiosis in the central nervous system (CNS) (Bruce and Dickson, 1987; Dickson et. al., 1968; Dickson et. al, 1984). However, the initial assumption that the causative agent was a slow-acting virus was disputed and attempts to modify, identify, or clone nucleic acids specific to PrP^{Sc} have failed to generate polynucleotides of significance (Kellings et. al, 1992; Meyer et. al., 1991; Oesch et. al. 1988; Prusiner, 1991).

Additional studies supporting the theory that PrP^{Sc} is devoid of nucleic acids emerged and several groups demonstrated that the agent in question was highly resilient to harsh treatments that are known to inactivate nucleic acids. In scrapie for example, researchers were unable to inactivate the infectious agent through many physical and chemical treatments such as boiling, freezing and thawing, formalin treatment, treatment with chloroform, and ultraviolet radiation (Alper, 1966; Alper et. al., 1966; Alper et. al., 1967; Pattison and Millson, 1961a; Pattison and Millson, 1961b; Pattison, 1965). In 1967 Griffith took this further and suggested that the transmissible agent was a protein (Griffith, 1967).

Despite this evidence, there was still speculation regarding this novel idea, in 1982, Bolton and colleagues were able to help solidify this theory when they successfully isolated a protease resistant sialoglycoprotein through proteinase K (PK) treatment of infected brain homogenate (Bolton et. al., 1982). The term “prion” was later coined and

defined by Prusiner as “small proteinaceous infectious particles that resist inactivation by procedures which modify nucleic acids” (Prusiner, 1982).

Prion Protein Isoforms

All of the four levels of protein structure (primary, secondary, tertiary, and quaternary), in addition to the environment, help to stabilize the folded, native conformation of a protein. Therefore, a protein is only functional when in its proper conformation and proper three-dimensional form. An inactive protein, with some exceptions, occurs when it is improperly folded or denatured often leading to its degradation.

In prion disease, the cellular form of the protein is converted into a new, β-sheet rich conformation that has an unknown tertiary structure. This is the conformation that causes disease. Therefore, all prion proteins exist in at least two distinct isoforms: the normal, cellular prion protein, PrP^{C} and the disease causing isoform referred to as scrapie or PrP^{Sc}. Moreover, a large body of evidence suggests that prion disease is mediated by the abnormal isoform, PrP^{Sc} (Prusiner, 1991).

Prion Protein Functions

While PrP^{Sc} is infection specific, PrP^{C} has some normal cellular functions. PrP^{C} is highly conserved in most mammals and is found in most adult tissues (Ford et. al., 2002). However, PrP^{C} is most prominently expressed in the CNS in synaptic membranes and within cells of the immune system as a glycosylphosphatidylinositol (GPI) anchored cell surface glycoprotein (Dodelet and Cashman, 1998). The normal function of PrP^{C} is

thought to include a role in oxidative stress, copper metabolism, synaptic structure, function and maintenance, cell adhesion, and trans-membrane signaling processes (Westergard et. al., 2007). However, the exact functions of PrP^{C} within these areas have yet to be clearly defined.

Conformational Properties of PrP^{C} and PrP^{Sc}

The two best approaches to analyze the atomic structure of proteins include nuclear magnetic resonance (NMR) and x-ray crystallography. Both approaches achieve high-resolution analysis of protein structure. However, NMR determines the structure of the protein in solution, often showing regions that are dynamic and unresolved, whereas x-ray crystallography looks at the structure in a static crystal form.

The conformation of PrP^{C} was first determined through NMR measurements made on recombinant mouse protein (Reik et. al., 1996). Since then, NMR structures have been determined for additional strains of the prion protein and have shown to consist essentially of the same conformation (Hosszu et. al., 1999; James et. al., 1997). Despite the efforts by several groups, determining the three-dimensional structure of PrP^{C} through x-ray crystallographic methods has not been successful. Furthermore, the insoluble properties of PrP^{Sc} have prevented successful determination of its structure by either x-ray crystallography or NMR methods. Therefore, our knowledge of PrP^{Sc} structure remains limited (Cohen and Prusiner, 1999).

Cellular Biology of PrP^{C} and PrP^{Sc}

In the first step of the secretory pathway, a new protein is translocated into the endoplasmic reticulum (ER) only after it has been fully translated in the nucleus. This process is called post-translational translation. Human PrP encodes a ~253 amino acid translational product that is moved into the ER. The first 22 amino acids of PrP code for a signal peptide and cause the mRNA/ribosome complex to move into the ER mid-translation. This process is referred to as co-translational translocation. These 22 amino acids are removed by signal peptidase from the N-terminus and PrP continues to be translated directly once it is in the ER. This occurs because a signal recognition particle (SRP) binds to and prevents the ribosome form continuing translation. Translation only continues when the ribosome/SRP complex encounters a SRP receptor and each bind to one guanosine triphosphate (GTP) molecule on the ER membrane. Once attached, translation continues pushing the signal peptide, and eventually the whole molecule of PrP into the lumen of the ER. Then, both the SRP and its receptor both hydrolyze their GTP and are released and the protein is free to start folding in the lumen. While the protein is still being translated, oligosaccharyl transferase (OST), adds glycosyl groups to asparagine residues in the nascent protein as a part of the translocon complex. PrP has 0, 1 or 2 possible sites on N-glycan consensus sequences, NXS and NXT (Harris, 2003).

The C-terminus of PrP is a 23 amino acid sequence that signals for the addition of a GPI anchor (Stahl et. al., 1987). In this process called glypiation, 23 amino acids are cleaved off and replaced with another type of sugar chain referred to as GPI. The GPI

then embeds into the membrane and anchors PrP to the ER. After cleavage of the signal peptide and the addition of the GPI anchor, human PrP becomes ~208 amino acids in length. Collectively, these processes produce a ~17kDa C-terminal fragment called C1 that is inserted into the plasma membrane of the cell and a ~9kDa unstructured and soluble N-terminal counterpart referred to as N1 that is released into the extracellular space (Chen et. al., 1995).

From the ER, GPI-linked PrP travels anterograde through the secretory pathway. It is transported in vesicles that bud off of the ER bound for the golgi apparatus for further modification and acquire a disulfide bond between its two cysteine residues C180 and C214 and also undergoes several modifications to its N-linked glycan chains. The golgi apparatus consists of a set of stacked sub-compartments called cinsternae that have different properties. These sub-compartments are celled cis, medial, and trans-golgi network and the modifications of proteins have to happen in a particular order within them. When proteins have finally completed maturation, they do one of three things. They either bud off in a vesicle and are exocytosed and fused with the cell membrane, get moved into secretory vesicles until needed, or they are placed into lysosomes if they are not correctly folded. Normally, PrP gets GPI-linked and delivered to the cell surface through an exocytic vesicle. Once there, it remains GPI-anchored to the surface of the cell membrane. Moreover, it has been shown that the majority of PrP on the cell surface is found within cholesterol and sphingolipid enriched domains (Hnasko et. al., 2010). However, there is evidence that PrP can exist in three membrane topologies including GPI-anchored and two trans-membrane orientations (Harris, 2003).

However, in pathological conditions, PrP^C undergoes an additional upstream cleavage of ~66 N-terminal amino acids (7kDa N-terminal peptide) and the persistence of a protease resistant core (C2) referred to as PrP 27-30 (Chen et. al., 1995).

Structural Features of PrP^C

The resulting, mature PrP^C isoform consists of two distinct parts. First, the unstructured N-terminal region of the protein contains a segment that includes five repeats of an eight amino acid sequence called the octapeptide repeat region and includes one binding site for copper ions thought to play a role in oxidative stress (Viles et. al., 1999). Studies on post-translational modifications show that PrP undergoes glycan addition at two asparagine (N)-linked glycosylation sites which occur on murine (mo) PrP at residues 180 and 196 (Bolton et. al., 1985; Oesch et. al., 1985).

Second, the C-terminus aspect of PrP at amino acids 121-231 encompassing murine PrP, is structured as it is folded into three α-helices and two, short β-pleated sheets. (**Fig. 2**). These are stabilized by a single, di-sulfide bond that links helices two and three (Reik et. al., 1996). In contrast to PrP^C, PrP^{Sc} has been shown by Fourier transform infrared spectroscopic methods to contain high β-sheet content but is indistinguishable from PrP^C in terms of sequence (Pan et. al., 1993; Stahl et. al., 1993).

Additional structural studies have shown that PrP^C is monomeric, sensitive to protease treatment, and is soluble in detergents (Wildegger et. al., 1999). In contrast, PrP^{Sc} is partially protease resistant, insoluble in detergents, and is highly aggregated forming

amyloid rods (Barry et. al., 1985; Meyer et. al., 1986). Treatment of PrP^{Sc} with proteinase K results in cleavage and the persistence of a protease resistant core PrP 27-30.

Prion Propagation and Recruitment

The molecular events that occur during infection which lead to the conversion of PrP^{C} to the diseased isotype, PrP^{Sc}, are still poorly understood. It is known that PrP^{Sc} is derived from PrP^{C} through post-translational modifications (Borchelt et. al., 1990; Caughey and Raymond, 1991). Though no differences between the amino acid sequence of PrP^{C} and PrP^{Sc} have been found, it was proposed that PrP^{Sc} acts as a template to promote the conversion of PrP^{C} to PrP^{Sc} through either a post-translational or conformational modification (Stahl et. al., 1993). Additional PrP^{C} molecules can then be recruited and lead to further conversion; which is dependent on the overall PrP^{C} concentration, resulting in the etiology of prion disease (**Fig. 1**) (Halliday et. al., 2014; Prusiner et. al., 1990; Telling et. al., 1995).

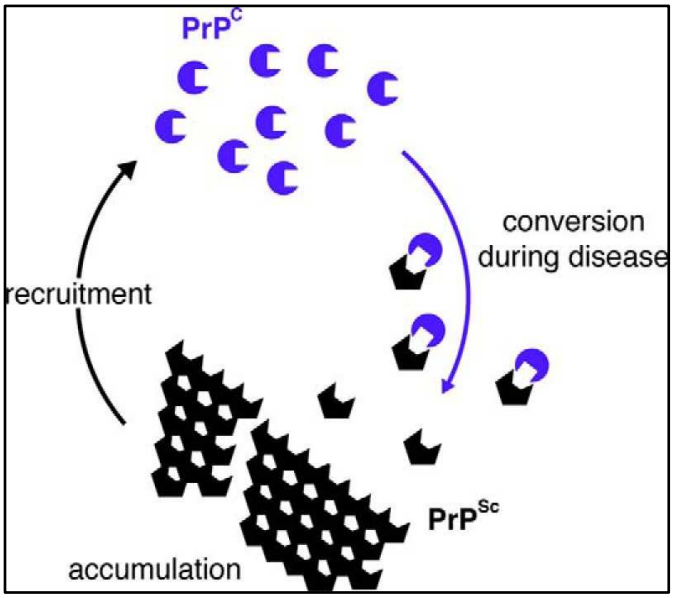

Figure 1. Schematic of Prion Conversion Native PrP^{C} (blue) is converted into PrP^{Sc} (black) through an autocatalytic process (Halliday et. al., 2014).

CHAPTER 2 – THE ROLE OF AGLYCOSYLATION IN MURINE PRION PROPAGATION

Introduction

N-Linked Glycosylation in PrP

Detecting TSEs does not come without difficulty as the most reliable confirmations of disease are performed post-mortem. Screening animals and humans for PrP^{Sc} is not possible as PrP^{Sc} is derived straight from the host and is not recognized by self as foreign. As a result, there is no adaptive immune response mounted during infection to activate T and B cells. This makes attempts to isolate PrP monoclonal antibodies (mAbs) challenging. Additionally, abnormal accumulation of PrP^{Sc} is concentrated in the brain and is difficult to detect in other bodily fluids and tissues (Kubler et. al., 2003).

Therefore, the gold standards for post-mortem detection of PrP^{Sc} include: a) immunohistochemistry (IHC), b) immunoblotting (WB), as well as c) bioassay of infected brain material into a susceptible host to demonstrate the transmission of infectious particles (Hadlow, 1999; Hnasko et. al., 2010; MacGregor, 2001; Pawel, 2004).

Consequently, to develop innovative diagnostics and treatments for prion diseases, it is important to gain a better understanding of the molecular mechanisms by which prions replicate and cause disease. It is therefore essential to grasp post-translational differences, such as glycosylation, between PrP^{C} and PrP^{Sc}, and the role they play in prion isotype conversion.

Historically, the role of N-linked glycosylation and its role in prion propagation has been a subject involving much controversy (Cancellotti et. al., 2007). N-linked glycosylation involves an enzymatic transfer of a lipid-linked carbohydrate onto the acceptor asparagine of the consecutive amino acid sequence that serves as the N-glycan recognition sequence: asparagine (N)-X-serine (S)/threonine(T), where X is any amino acid other than proline (P). PrP has two highly conserved sites for N-glycan attachment at murine residues 180 and 196. Occupancy at these two sites yields four different glycotypes: fully-glycosylated PrP (di-glycosylated), as well as three under-glycosylated forms including mono-glycosylated at 180 (mono-1), mono-glycosylated at 196 (mono-2), and completely aglycosylated with no glycan attachment at either site. N-linked glycosylation is one of the most common post-translational modifications of extracellular membrane proteins and results in great functional diversity of proteins including protein folding, stability, and aggregation (Hanson et. al., 2009; Mitra et. al., 2006).

Mapping Functional Epitopes

The involvement of specific amino acid residues in conformational epitopes and their effects on PrP during infection have only just begun to be defined. There is an advantage to understanding the involvement of specific amino acid residues in discontinuous, conformational-dependent PrP epitopes as it could provide a means to better understanding PrP biochemically both in structure and interactions and can pave the way for potential diagnostics and therapeutics.

Earlier studies by Kang and colleagues (Kang et. al., 2012) aimed to define the involvement of specific amino acid residues in discontinuous, conformation dependent PrP epitopes and their role in prion propagation. These studies used shuffled genes expressing novel PrP epitopes to determine the reactivities of the resulting mAbs against a large panel of PrP primary structures and polymorphic variants. The goal was to map out and confirm by mutational analysis the involvement of specific residues on epitope binding and PrP^{C} to PrP^{Sc} conversion (**Fig. 2**).

Results show that binding of one monoclonal antibody in particular, PRC7, is sterically prevented by N-glycan occupancy at residue N196 on the murine PrP (mono-2) and as a result, recognizes only the mono-1 and aglycosylated species of PrP (Kang et. al., 2012). Through additional studies it was shown that PRC7 recognizes a discontinuous epitope on murine PrP that includes Y154, Q185, and F197 in the globular region of the protein and requires proximity in the folding of the tertiary structure of PrP for recognition. Furthermore, these studies showed that PRC7 reactivity of PrP increases during infection and thus mono-1 or aglycosylated PrP could be specific to PrP^{Sc}.

Other mAbs of significance to mention include PRC5 and D13. The former recognizes a discontinuous epitope on murine PrP including A132 and N158 in the globular region and like PRC7, also requires proximity for recognition in the tertiary structure of the PrP^{C}. Unlike PRC7, immunoreactivity to this mAb does not increase during infection. Because of its location and properties, PRC5 acts very similar to the widely studied 6H4 mAb with the exception that 6H4 recognizes a linear epitope at amino acids 144-152

(Kang et. al., 2012; Korth et. al., 1997). Finally, mAb D13 consists of a continuous, linear epitope upstream of the globular region of murine PrP at 94-105 and does not depend on the tertiary structure of the protein for recognition and is not specific to infection (unpublished data Kang et. al.; Matsunaga et. al., 2001).

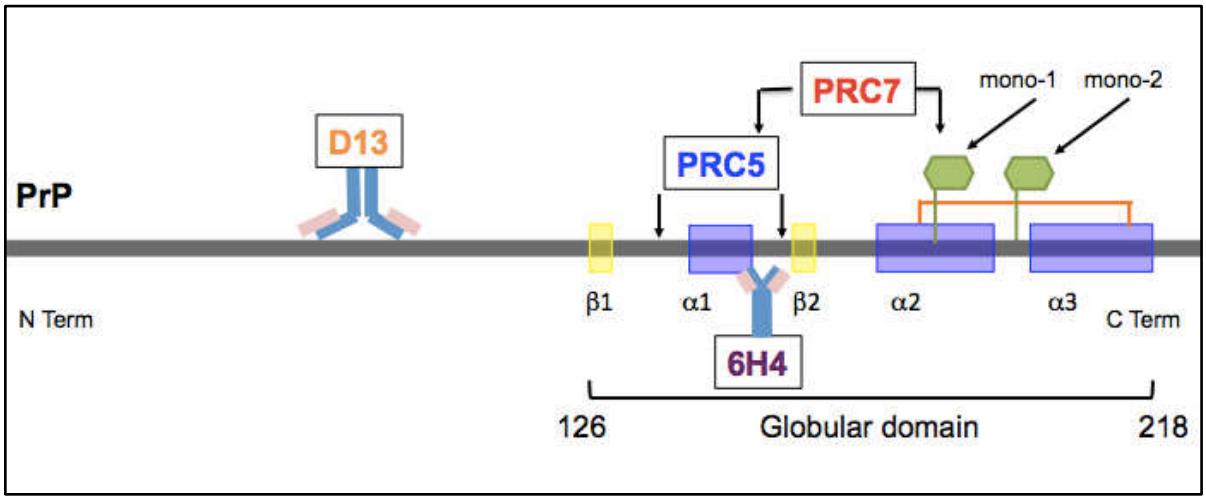

Figure 2. Mapping of mAbs Generated Murine PrP shown with mAbs of significance in this body of work and where their epitopes are located along the protein. Figure adapted from Kang, HE.

These data suggest that conversion of PrP^{C} to PrP^{Sc} depends largely on its state of glycosylation. Additionally, these data also provide a means of distinguishing PrP^{C} from PrP^{Sc} immunologically, without reliance on protease treatment and provide an option for use in WB, IHC, and other assays in the future.

Systemic Mutation of N-Glycan Attachments on Murine PrP

Preliminary Data – Mono-2 Substitutions

In preliminary, unpublished studies by Kang and colleagues, an innovative molecular genetic method was used as a way to remove N-linked glycosylation at residue 196 and

the downstream T at 198 on murine PrP in order to systematically study the role of underglycosylation in prion propagation. These studies mutated the N at glycan residue 196 and the T at site 198 to each of the remaining 19 amino acids individually. Thereafter, these constructs were stably transfected into Rabbit Kidney Epithelial cells (RK13), which do not endogenously express PrP (Vilette et. al., 2001).

Through immunoblotting and probing with PRC5 and PRC7, results showed that these mutations did not affect the ability of the globular domain to attain the appropriate tertiary structure required for the recognition of PrP^{C} (**Fig. 3**). Additionally, as expected, detection with PRC5 showed that all mutations prevented the formation of di-glycosylated PrP by preventing glycosylation at 196. The resulting immunoreactive bands included a ~27kDa unglycosylated full length PrP and its ~33kDa monoglycosylated counterpart, mono-1; as well as a ~17kDa C1 fragment and its ~22 kDa monoglycosylated counterpart (**Fig. 3**). The two exceptions to these results include substitutions N and S made at 198 in which the fully di-glycosylated form of PrP was also produced. This can be easily explained by the fact that the third residue required for N-glycosylation attachment can be either an S or a T. Moreover, because residue 200 is a T, the T198N mutation creates an additional cryptic N-glycan attachment site (**Fig. 3**).

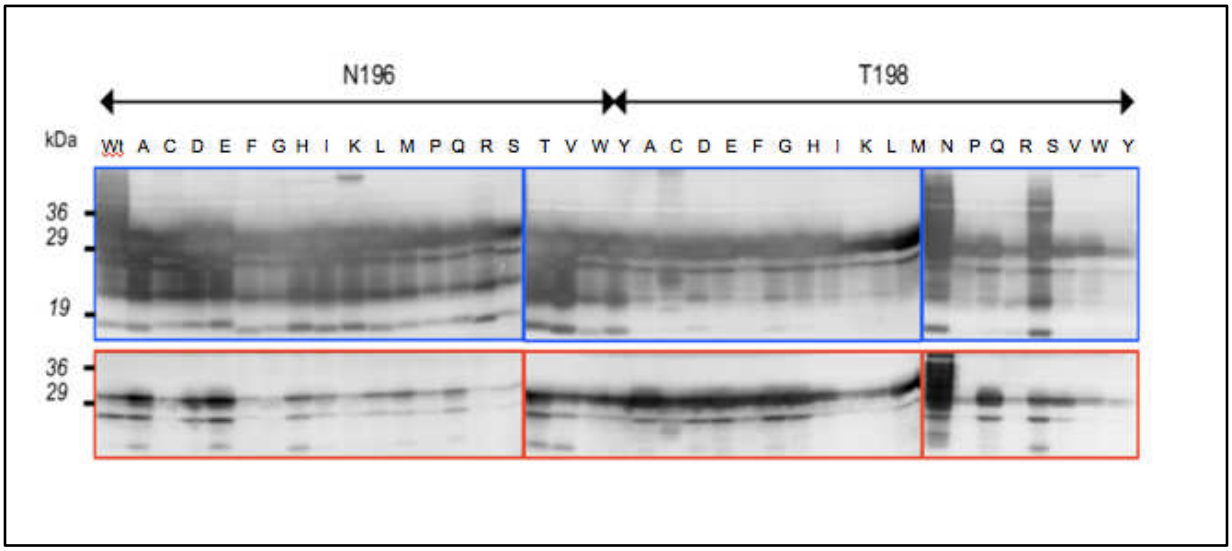

Figure 3. Mono-2 Glycan Site Mutation Western Blots Probed with PRC5 and PRC7 N196 and T198 site mutations in mo PrP are shown. Blots were probed with mAbs PRC5 (blue boxes) and PRC7 (red boxes). All samples containing glycan substitutions showed detection of all PrP glycoforms and their derivatives as predicted with the exceptions of T198N and T198S. Data generated by Kang, HE.

After confirmation of PrP^{C} expression of these constructs, these mutant cells were subsequently infected with prion isolates RML, 22L, 139A, and mCWD. Following four-weeks of infection, cells were counted and plated onto ELISpot plates, immunodetected with 6H4; a widely used, commercially available mAb (Thermo Fisher Scientific, Cat. #7500997) with a linear epitope located at amino acids 144-152 on PrP (Korth et. al., 1997; McCutcheon et. al., 2014), and spots from single cells were counted. Outcomes show that substitutions at both N196 and T198 exhibited variability between each of the prion isolates with the exception of lysine (K) at 196, in which prion propagation was detected in all four (**Fig. 4**). Because of this interesting result, N196K will be the focus for future studies.

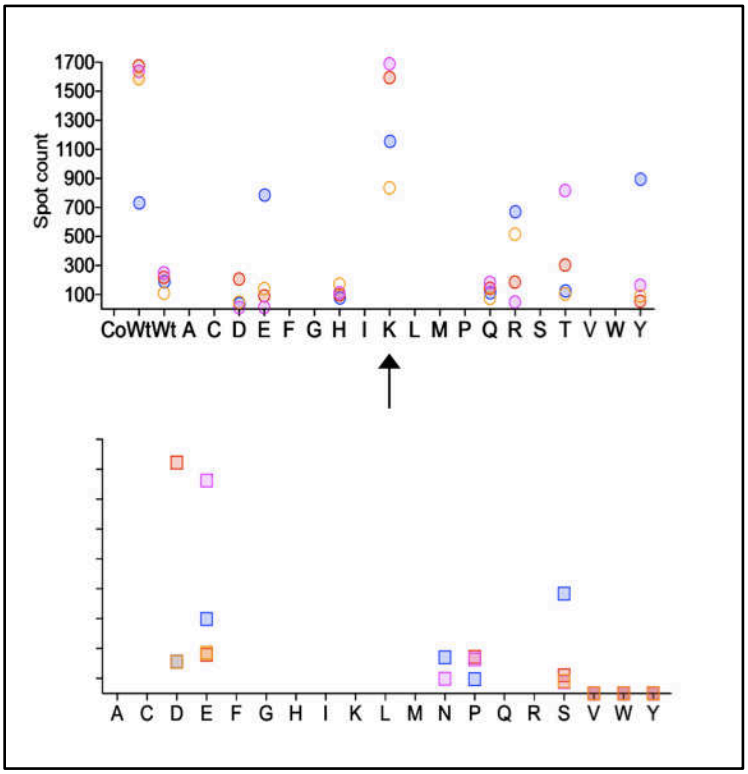

Figure 4. Scrapie Cell Assay PrP^{Sc} production in different murine prion isolates RML (blue), 22L (red), mCWD (magenta), and 139A (orange) for N196 (circles) and T198 (squares) site substitutions. Each mutant was infected and plated along with controls; cells containing the empty vector (Co), cells expressing WT mo PrP chronically infected with RML (first Wt), and freshly infected cells expressing WT mo PrP (second Wt) onto ELISpot plates 4-weeks after infection. Detection of infected cells was done using mAb 6H4. Prion propagation was variable between both mutation sites and isolates tested with the exception of the lysine (K) substitution at N196 (arrow), in which all four isolates provided propagation. Data generated by Kang, HE.

Even though N196K supported the conversion of PrP^{C} to PrP^{Sc} by allowing prion propagation, this same mutation may not have similar effects on the second glycan attachment site, at residue N180 (mono-1) or its recognition sequence, S/T182. This is primarily because the mono-1 and mono-2 consensus sequences (NXS/T) occur in very different areas of the primary and secondary structures of PrP^{C}. Mono-2 is located in the linker region that connects α-helices two and three while mono-1 is positioned within

α-helix two. Therefore, it is important to first investigate the role of these same amino acid substitutions at mono-1 during prion infection in order to proceed with further studies thereafter.

The strategies started by Kang and colleagues to study each amino acid substitution at both mono-1 and mono-2 are continued in this body of work. These studies take a unique approach to studying the role of glycosylation in prion propagation by addressing each N-glycan attachment sequence on PrP with individual amino acid changes. This is essential because each of the glycan attachment sites on PrP is located in unique areas of the protein and may affect prion propagation differently.

Introduction to this Body of Work

In this body of work, I continued the efforts performed previously by Kang and colleagues by investigating the effects of amino acid mutations at the N180 glycan site (mono-1) on murine PrP in prion propagation. I utilized one of the gold standards, immunoblotting, as my readout for baseline PrP^{C} detection as it remains a reliable, widely accepted molecular technique. The readout for prion propagation, known as the scrapie cell assay (SCA), was used following infection with several lysates. In addition, I also used the same laboratory-generated monoclonal antibodies as they provide a new, promising tool for prion detection.

Overarching Hypothesis and Specific Aims

My central hypothesis is that an underglycosylated form of PrP is preferentially generated during prion propagation.

Specific Aim 1: Investigate the relationship of individual mono-1 mutations on murine PrP by analyzing their effects on PrP^C expression.

Specific Aim 2: Address which substitutions at mono-1 are of significance in murine prion propagation using four prion isolates.

Experimental Procedures

Generation of Constructs

PrP coding sequences with or without single mutations for each of the 19 amino acids at N180 or S/T182 of the murine PrP transcript variant 1 mRNA sequence (NCBI reference sequence, NM_011170.3) were synthesized (GeneScript, NJ) in a pIRESpuro.3 vector (Clonetech, Cat. #631619) with only a single restriction endonuclease recognition sites for each AflII and EcoRI at 5' and 3' respectively and ampicillin resistance (**Fig. 5A,B**). Ligations were transformed into Top10 chemically competent *E. coli* cells (Invitrogen, Cat. #C404006) according to the provided chemical transformation protocol and grown on agar plates with ampicillin (100 µg/mL) at 37ºC overnight.

A

	CAG	AAC	AAC	TTC	GTG	CAC	GAC	TGC	GTC	AAT
171	Q	N	N	F	V	H	D	C	V	**N**
	ATC	ACC	ATC	AAG	CAG	CAC	ACG	GTC	ACC	ACC
181	I	T	I	K	Q	H	T	V	T	T
	ACC	ACC	AAG	GGG	GAG	AAC	TTC	ACC	GAG	ACC
191	T	T	K	G	E	**N**	F	T	E	T

B

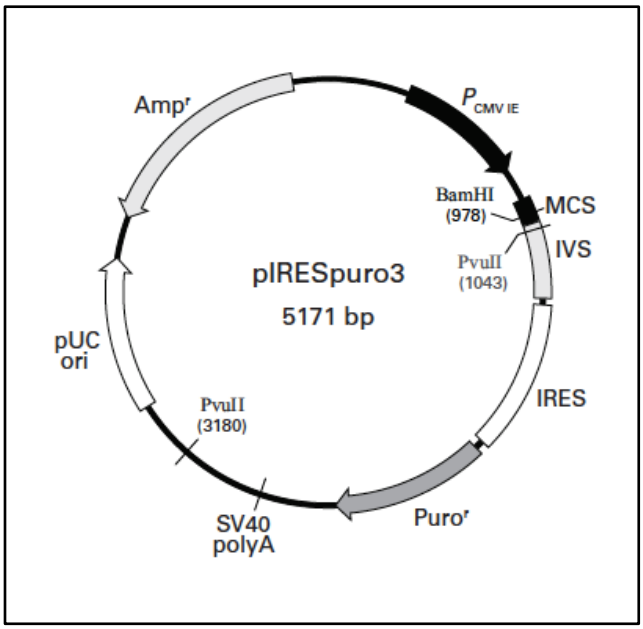

Figure 5. Generation of Mutant Constructs Sequences containing individual amino acid mutations at N180 and S/T182 of the N-glycan consensus sequence were designed on murine PrP. N180 represents the mono-1 attachment site and is shown in red along with N196 site for mono-2 **(A)**. Mutations were then inserted into a PIRESpuro.3 vector **(B)**. Vector image obtained from Clonetech.

Single colonies were immediately selected and inoculated into 3mL of Luria (LB) broth containing 100µg/mL ampicillin and expanded for 12-18hrs at 37ºC with agitation. The next day, glycerol stocks were made using 500µL of culture and 500µL of 50% glycerol and frozen at -80ºC for long-term storage.

Plasmid DNA was then isolated from the remaining construct cultures using the QIAprep Spin Miniprep Kit (Qiagen, Cat. #27104) and concentrations were measured using a NanoDrop 2000c Spectrophotometer (Thermo Scientific). At the same time, samples were checked for acceptable salt contamination (260/230) and purity (260/280) ratios of ~2.0 and 1.9 respectively (Thermo Fisher Scientific, 2009).

Confirmation of Constructs

To confirm that all constructs generated contained the appropriate plasmid and insert, restriction digests using EcoRI and AflII were set up using 1µg of plasmid DNA, 1µL of each restriction enzyme, 3µL of 10x Buffer (NEB), and brought up to a volume of 30µL with dH_2O. These mixtures were then incubated at 37ºC for 1-hour, DNA fragments separated on a 0.8% agarose gel containing EtBr at 100V for 1-hour, and visualized by ultraviolet (UV) light box. Results show that two products form, one at the expected plasmid length for pIRESpuro.3 at ~5171bp and one at the insert length at ~777bp (**Fig. 6A,B**).

A

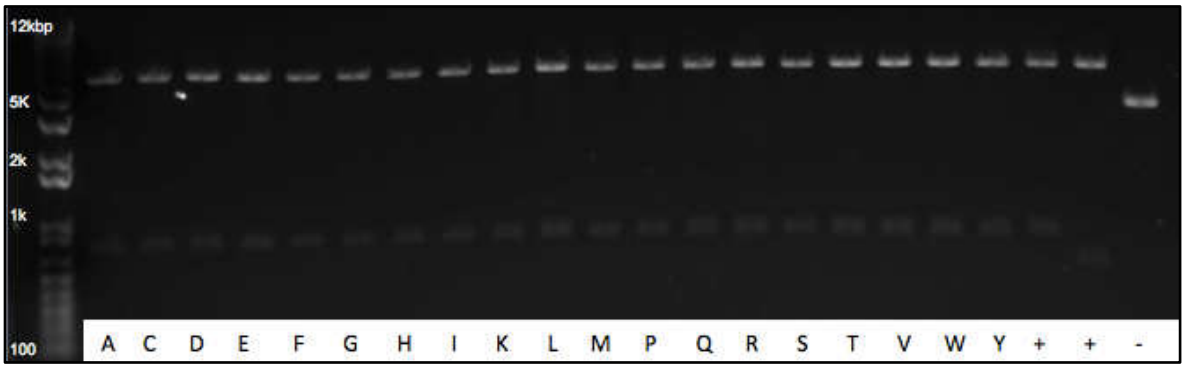

B

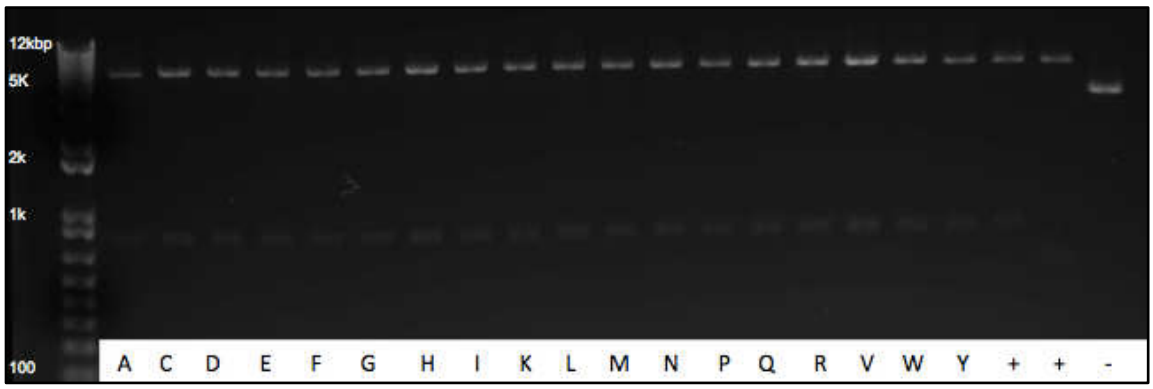

Figure 6. Digested DNA from Generated PrP Mutants DNA from N180 **(A)** and S/T182 **(B)** mutant cells digested with restriction enzymes EcoR1 and AflII. Results confirm two bands, one at the vector length at ~5171bp and one at the insert length at ~777bp.

Additionally, 1µL of undigested DNA from all constructs were separated on a 0.8% agarose gel containing EtBr at 100V for 1-hour, and visualized using a UV light box to determine the relative ratios of naked/circle, linear, and supercoiled DNA (red boxes). Supercoiled is the native form of DNA found *in-vivo* and occurs when extra twists are introduced into the double helix strand. Furthermore, supercoiled DNA is the desired species when isolating plasmid DNA to use for stable transfections because this species results in greater transfection efficiency, increasing the chances of a stable transfection (Cherng et. al., 1999). Results confirm that each DNA species is present in all construct DNA samples with supercoiled DNA at an acceptable relative ratio to proceed with transfections (**Fig. 7A,B**).

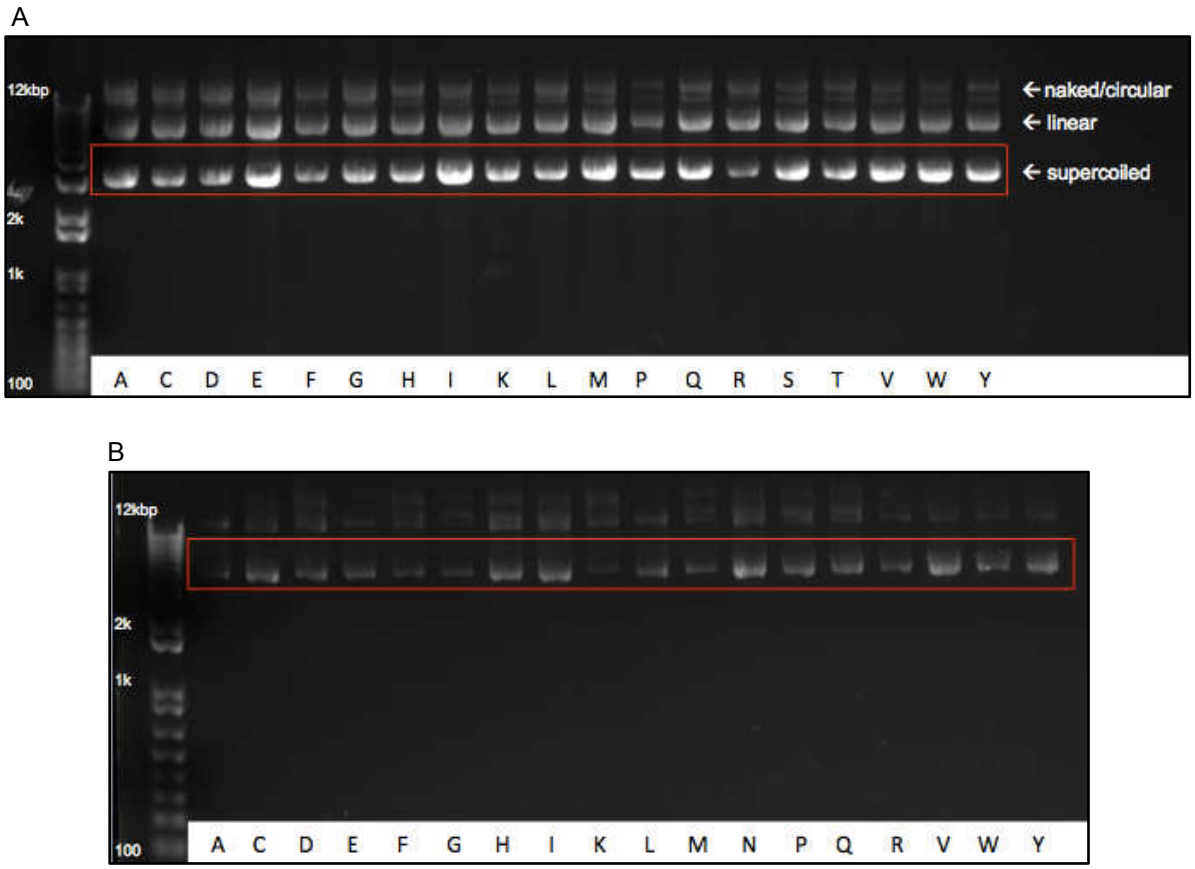

Figure 7. Undigested DNA from Generated PrP Mutants DNA from N180 **(A)** and S/T182 **(B)** mutant cells. Results show the relative ratios of naked/circle, linear, and supercoiled DNA. Supercoiled DNA is the species of interest for stable transfections (red boxes).

Transfections

Following confirmation that satisfactory plasmid DNA was generated to use for transfections, Rabbit kidney epithelial cells (RK13) previously obtained from the American Type Culture Collection (ATCC, Cat. #CCL-37) were transfected in bulk with random insertion of plasmid (pIRESpuro.3) DNA containing murine wild-type (WT), altered murine PrP sequence, or empty vector to produce RKM (RKM 1-3), RK13 mutants, and RKV cells respectively.

One day prior to transfection, RK13 cells were counted and $4x10^5$ cells/well were plated onto 6-well tissue culture (TC) plates in 2mL of media without antibiotics. The following day, transfection mixtures were prepared by mixing 2µg of plasmid DNA and 3.4µL of Lipofectamine 2000 (Invitrogen, Cat. #11668019) into a total of 1000µL of OptiMEM (Gibco, Cat. #31985070) and plated onto the cells. Following a 5-hour incubation at 37ºC, 2mL of complete DMEM medium (HyClone, Cat. #SH30022.01) containing 1µg/mL penicillin/100 U/mL streptomycin and 10% FBS (Peak Serum, Cat. #PS-FB1) was added. The next day, cells were trypsinized (HyClone, Cat. #SH30236.01) and transferred into $10cm^2$ TC dishes containing 10mL of complete DMEM and maintained in 37ºC with 5% CO_2.

Puromycin (puro) (Sigma Aldrich, Cat. #P8833) selection began 24-hours later at a concentration of 1µg/mL and was refreshed every 2-4 days. Death of cells lacking the plasmid insert began a few days post-transfection and continued through to ~1.5 weeks in no vector controls.

Successful visualization of single colonies in all cells containing the vector (RKM, RK13 mutants, and RKV) began around 1-week post-transfection and continued as dishes grew to confluency. At this time, all constructs were split into three, $10cm^2$ TC dishes to a) be frozen down in DMEM without antibiotics containing 10% DMSO for later use, b) harvested for protein for western blot analysis (WB), and c) maintained in complete DMEM with puromycin to be used for prion infections and to be later analyzed by SCA on ELISpot plates.

Western Blot Analysis

To determine the base-line expression levels of the PrP^C, cell pellets of all constructs were individually lysed in 200µL of cold lysis buffer (CLB) containing 50mM Tris pH 8.0, 150 mM NaCl, 0.5% sodium deoxycholate, 0.5 igpal CA-630 and analyzed through western immunoblotting.

Protein concentrations of cell lysates were determined by bicinchoninic acid assay (BCA) (Pierce, Cat. #23225). Aliquots containing 50µg of total protein were prepared for SDS-PAGE, and boiled for 10-minutes prior to loading. Proteins were separated on 18-well, Criterion XT 12% acrylamide gels (Bio-Rad, Cat. #3450118) and transferred to polyvinylidene difluoride immobilon (PVDF)-FL membranes (EMD Millipore, Cat. #IPFL00010). Membranes were blocked with a 1:1 dilution of casein blocking solution (LI-COR, Cat. #927-40200) in 1x Tris-buffered saline with 0.1% Tween-20 (TBST) and probed with each of the primary mAbs of interest (PRC5, PRC7, and D13) and GAPDH loading control in TBST at 4ºC overnight with agitation. Membranes were washed in TBST for three consecutive, 10-minute intervals at room temperature with agitation followed by incubation for 1-hour at room temperature with the appropriate fluorescently tagged secondary antibody (LI-COR). Membranes were washed again and protein bands were visualized by immunofluorescence using a LI-COR Oddesy CLx imaging system.

PrP Strains

It has been accepted that lesion profiling/vacuolation scoring, electrophoretic mobility, incubation times, among others, are reliable methods for prion strain typing (Angers et. al., 2010; Bessen and Marsh, 1992; Kovacs et. al., 2013). And as such, these different strain dependent features can be a consequence of different tertiary structures of the PrP^{Sc} molecules.

In this body of work, RML, 22L, 139A, and mCWD murine-adapted strains were used for infections. RML, 22L, and 139A are distinct, biologically cloned prion strains that originate from sheep scrapie (Bruce et. al., 1991), whereas mouse-adapted CWD is derived from chronic wasting disease prions in mule deer (Sigurdson et. al., 2006).

Ethics Statement

Mice were bred and maintained at Lab Animal Resources at CSU. This facility is accredited by the Association for Assessment of Lab Animal Care International in accordance with protocols approved by the Institutional Animal Care and Use Committee at CSU (IACUC Protocol #17-7266A). Mice were humanely euthanized using CO_2 inhalation.

Mice

All mice used in this body of work were originally purchased from The Jackson Laboratories and maintained and bred at CSU.

Preparation of Brain Homogenates for Infection

Prion infected and uninfected mice were euthanized and brain samples were harvested and frozen at -80ºC. Brain homogenates (BH) were prepared in 10% weight (g)/volume (mL) in sterile, 1x phosphate buffered saline (PBS). Samples were then homogenized via FastPrep-24 (MP Biomedicals) with glass beads in the tubes at maximum speed for three; 20-second intervals with three 5-minute rests on ice in between. After homogenization, samples were aliquoted and stored at -80ºC for later use.

Prion Infections

Frozen aliquots of 10% normal brain homogenate (NBH) samples from uninfected FVB/N mice, as well as RML, 22L, 139A, and mCWD infected mice were used to make 0.1% dilutions in sterile, 1x PBS. Each BH at 100µL/well was coated onto 96-well TC plates in triplicate for each cell of interest and left to incubate inside a TC hood for 1-3-hours at room temperature. Homogenates were then aspirated off and wells were washed twice with 200µL/well of sterile, 1x PBS and aspirated off. Plates were then left to dry completely in the TC hood before they were covered in saran wrap and stored at 4ºC until they were needed.

Wild-type RKM, RK13 mutants, RKV, and RKM7, a highly sensitive, single cell clone containing the murine wild-type PrP gene, were trypsinized, counted, and re-suspended in complete DMEM with 1µg/mL puromycin and plated at 20,000 cells/100µL/well onto 96-well TC plates containing prion isolates or NBH as described above. Cells were then

left to incubate at 37ºC in 5% CO_2 for 4-weeks. Complete cell culture medium with puromycin (150µL) was changed every 5-days.

Scrapie Cell Assay

To elucidate which murine PrP N-glycan substitutions play a significant role in prion propagation in prion isolates RML, 22L, 139A, mCWD, and NBH control, the SCA was used as a highly immunosensitive means to measure the frequency of PrP^{Sc} secreting cells at the single-cell level.

Enzyme-linked immunospot (ELISpot) plates (EMD Millipore, Cat. #MSIPN4W50) were activated with 70% ethanol and washed three times with 1x PBS, the last wash being left on the plates. Cells of interest in a 96-well TC plate were washed once with trypsin, aspirated, and fresh trypsin was added. Cells were incubated at 37ºC for 5-20 minutes or until cells were detached. Cells were counted and re-suspended in complete DMEM, and plated at 20,000cells/100µL/well onto the prepared ELISpot plates containing 1x PBS as shown in the NBH examples for each of the corresponding construct locations and lysates (**Fig. 8A,B**). A vacuum was applied to remove media, and plates were washed twice with 1x PBS. Plates were placed in a 50ºC oven for 1-hour or until completely dry, wrapped in plastic wrap, and stored at 20ºC overnight.

A

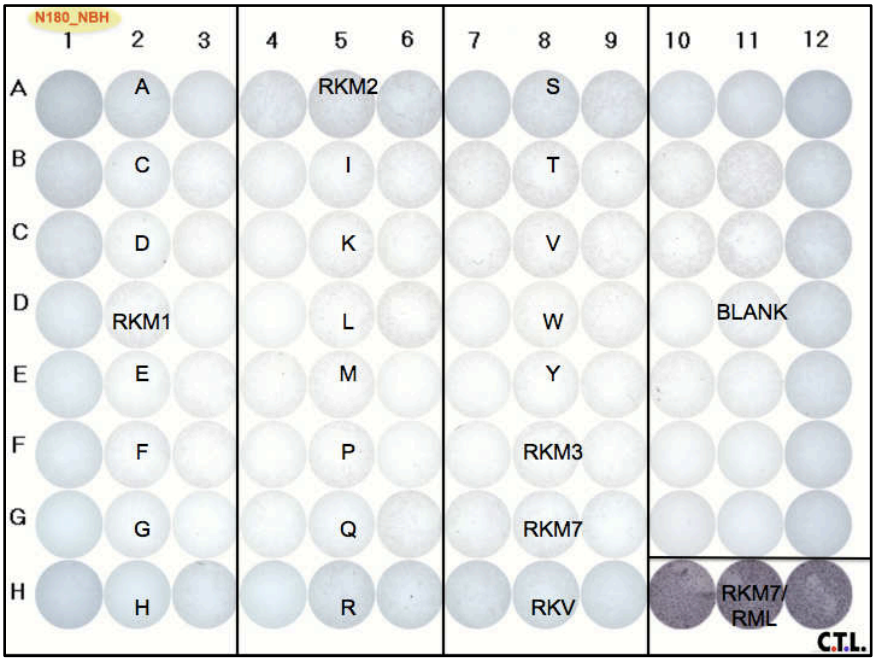

B

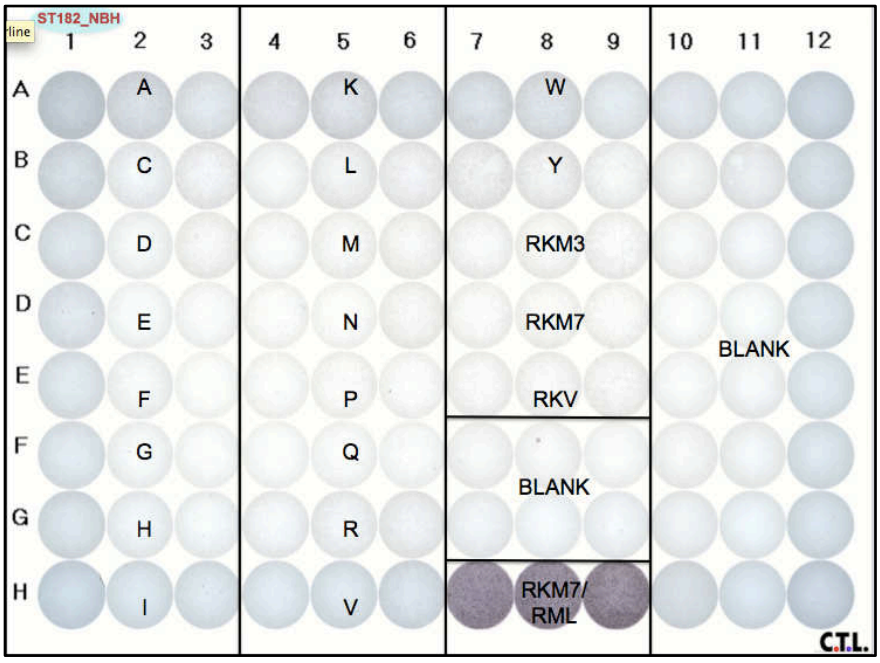

Figure 8. ELISpot Plate Layout SCA and analysis layout examples for each of N180 **(A)** and S/T182 **(B)** incubated with NBH (shown), RML, 22L, 139A, or mCWD isolates. Samples were transferred directly from 96-well plates that were infected in triplicate for 4-weeks.

Immunodetection of experimentally infected RKM, RK13 mutants, RKV, and RKM7 cells on ELISpot plates was performed as previously described (Bian et. al., 2010; Bian et. al., 2014) using mAb D13, and scanned with Immunospot S6UNIV equipment (Cellular Technology Limited). Spot numbers were then determined by using Immunospot 5.0 Analysis and 5.1 Counting software (Cellular Technology Limited).

Conformation of Murine PrP N-Glycan Mutations through Genetic Sequencing

To determine if the mono-1 constructs generated were both accurately and correctly inserted into RK13 cells, polymerase chain reactions (PCR) were set up for a few of the constructs using primers designed through Integrated DNA Technologies (IDT) to amplify either the cytomegalovirus (CMV) promoter in vector pIRESpuro.3 as a positive control, or murine PrP encompassing the mutations at sites 180 and 182 using pIRESpuro.3.

For each PCR reaction, 12.5 µL of GoTaq master mix (Promega, Cat. #M7122) was used in combination with 1.25µL of each forward and reverse primer set at concentrations of 10µM each and brought up to 22µL with PCR-grade water. Then, 500ng/3µL of each DNA template to be tested was added, totaling a 25µL/PCR reaction. Tubes were then placed in a Thermocycler (Bio-Rad) detailing a protocol specific to the primer design, amplified, and 8µL of the reaction was separated by electrophoresis on a 0.8% agarose gel at containing EtBr at 100V for 1-hour for product visualization using a UV light box.

After confirming the appearance of single bands at the correct size (~820bp for murine puromycin PrP and ~351bp for CMV), remaining PCR products were purified using a QIAquick PCR Purification Kit (Qiagen, Cat. #28104), quantified using a NanoDrop 2000c Spectrophotometer (Thermo Fisher Scientific), and checked for acceptable salt contamination (260/230) and purity (260/280) ratios of ~2.0 and 1.9 respectively (Thermo Fisher Scientific, 2009). Sequencing primers were designed to flank the mutated region to provide reads on the forward and reverse strands. Samples were then sent for sequencing to GENEWIZ, NJ according to the instructions provided. Results showed that the construct DNAs tested were the correct mutations at the correct site, confirming the successful generation of glycan substitutions at residues N180 and S/T182 on murine PrP in RK13 cells.

Results

Western Blot Analysis

Western blots have traditionally been used as a reliable readout to detect prion disease post-mortem (Hadlow, 1999; Hnasko et. al., 2010; MacGregor, 2001; Pawel, 2004). Therefore, we set out analyze immunoreactive bands for both N180 and S/T182 site substitutions of the consensus sequence of PrP to confirm mono-1 N-glycan ablation and verify PrP^{C} expression including PrP glycoforms.

Data from western blot analysis of substitutions at the N180 site on murine PrP showed that all substitutions, with the exception of proline, exhibited immunoreactive bands at mono-2 full-length, aglycosylated full-length, the mono-2 C1 fragment, and the

aglycosylated C1 fragment when membranes were probed with mAb PRC5 (**Fig. 9A,C**). Moreover, these mutations were confirmed to result in the ablation of N-glycan attachment at mono-1 of murine PrP as shown by the absence of the di-glycosylated glycoform (**Fig. 9A**). Because it is well known that the properties of P causes a disruption in amino acid structure, it can be assumed that P affects N-glycan attachment of these mutant cells and can explain the absence of all other bands, except mono-2 full-length PrP which was detected. Additionally, these same N180 constructs, with the exception of P in which there was a complete absence of banding pattern, showed bands consistent with aglycosylated full-length PrP and its derivative, aglycosylated C1 when stained with PRC7 (**Fig. 11A,B**). These results confirm the successful generation of mono-1 PrP mutants and resulting underglycosylation. They also verify the specificity of mAb PRC7 for mono-1 because mono-1 is ablated in all of these mutants and no band was detected for mono-2 full-length or its derivative, C1. Lastly, detection of all PrP glycoforms, excluding the C1 derivative, was shown in all substitutions, excluding P, when stained with mAb D13 (**Fig. 13A,B**). This is explained by the fact that C1 is cleaved upstream of the D13 epitope and therefore could not be detected.

Interestingly, results from western blot analysis of substitutions at the murine PrP S/T182 site did not yield any immunoreactive bands with either PRC5 or PRC7 (**Figs. 10A,C; 12A,B**). It can be hypothesized that these results are due to the fact that the discontinuous epitope for PRC7 is a component of mono-1, and the discontinuous epitope encompassing PRC5 is just upstream of mono-1 in the globular region of PrP. This means that altering the amino acid structure at either site on mono-1 can result in

the misfolding of PrP^C, which sterically prevents the detection of these mAbs in the S/T182 mutations (**Fig. 2**). Moreover, these data also suggest that S or T constitute part of the epitope recognized by PRC5 and PRC7. These results can also be explained by the possibility that during processing, PrP in the S/T182 mutants gets flagged by the golgi apparatus and gets caught in the cytoplasm of the cell and is unable to be fully-processed and sent to the cell surface for expression and detection. Furthermore, mono-2 full-length bands were recognized by mAb D13, which is located upstream of the globular region in these mutant cells (**Fig. 2**). These results further demonstrate that PrP is expressed at some level in the S/T182 mutations but may not be transported to the cellular surface. Interestingly, there was also doublet identified in the N mutation with the D13 mAb (**Fig. 14A,B**). This doublet shows mono-2 full-length bands that are similar in size to those of the N180 mutants. The sequence of the S/T182N mutant was checked to confirm that there was not a downstream cryptic consensus motif. Analysis of the amino acid sequence of the mutation shows that the N substitution does not result in a cryptic glycosylation site as the downstream amino acid at 184 is K, not the S/T that is required for the consensus sequence (**Fig. 5**).

A

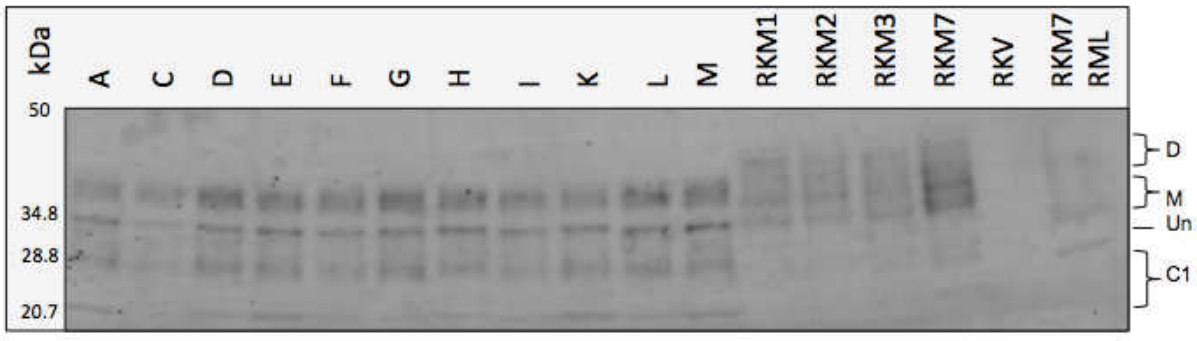

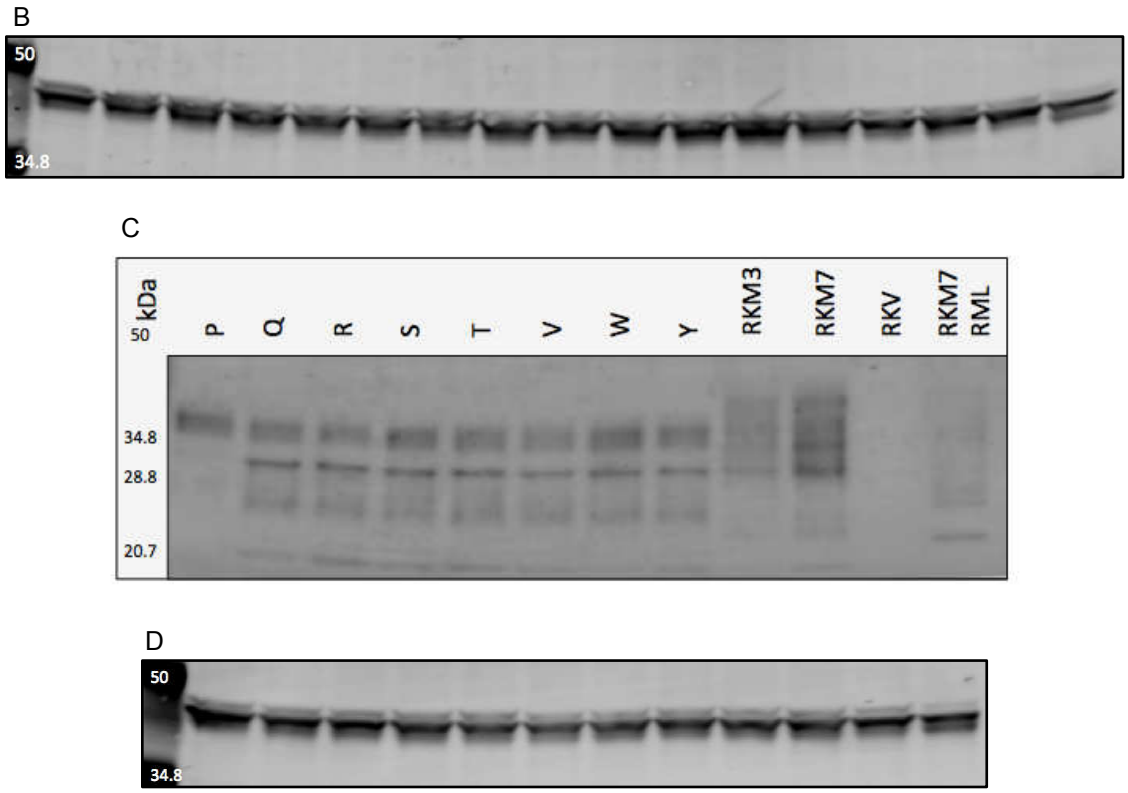

Figure 9. Representative N180 Site Mutation (Mono-1) Western Blots Probed with PRC5 and GAPDH N180 site mutations in mo PrP are shown along with controls including freshly infected cells expressing WT mo PrP (RKM 1-3), a highly expressive clone expressing WT mo PrP (RKM7), cells containing the empty vector (RKV), and RKM7 cells chronically infected with RML (RKM7/RML). Samples (50µg total protein) were run twice to confirm bands and probed with mAbs PRC5 at 1:5000 **(A)** and **(C)**, and GAPDH at 1:3000 **(B)** and **(D)**. All samples containing glycan substitutions with the exception of proline (P), showed detection of all PrP glycoforms and their derivatives, as predicted. For all western blots in this body of work, the immunoreactive bands labeled in (**A)** as D=diglycosylated full-length, M=monoglycosylated (mono-2) full-length, Un=aglycosylated full-length, C1=derivative fragments of monoglycosylated and aglycosylated). All samples were evenly loaded as shown by GAPDH band intensity.

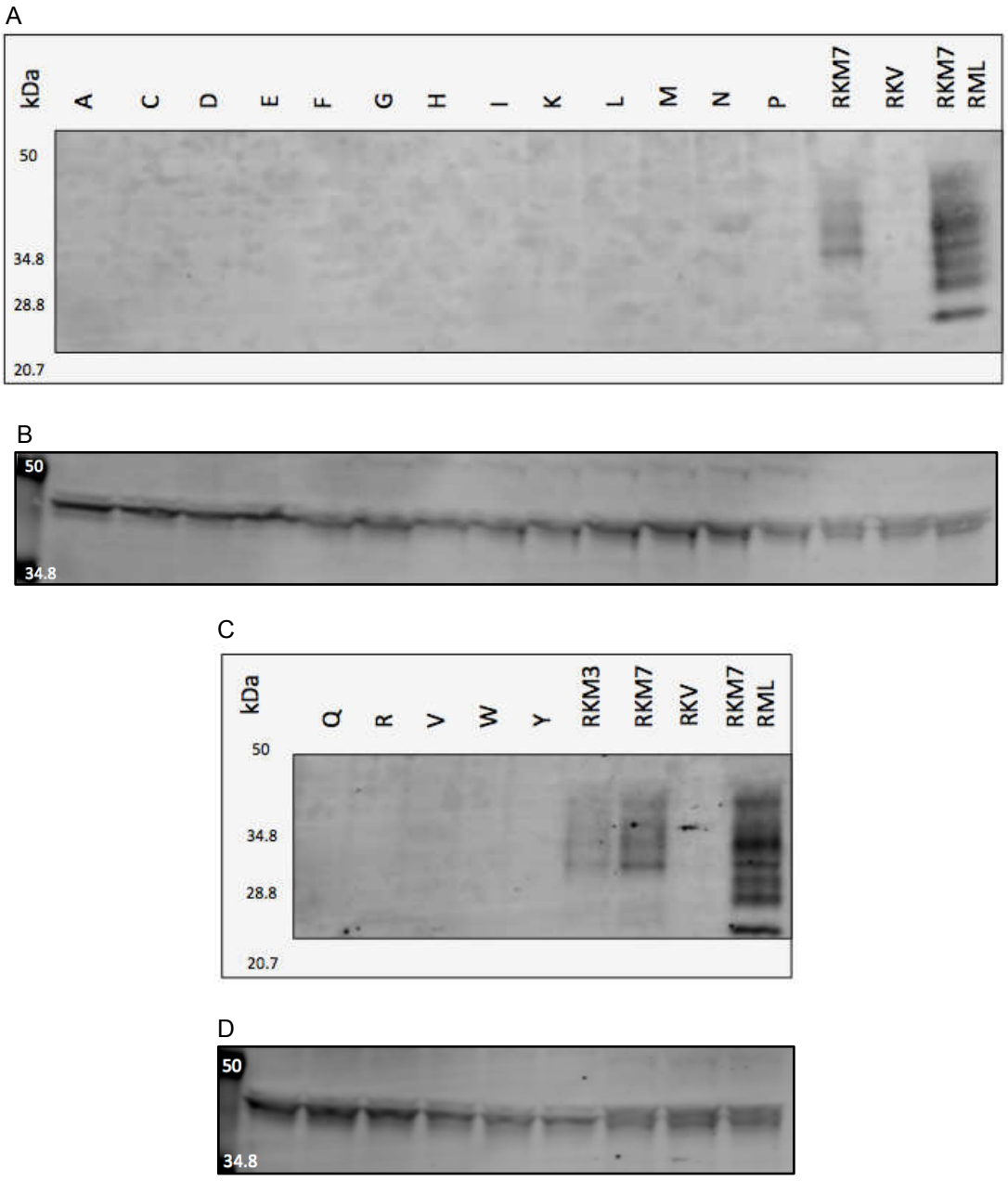

Figure 10. Representative S/T182 Site Mutation (Mono-1) Western Blots Probed with PRC5 and GAPDH ST182 site mutations in mo PrP are shown along with controls including freshly infected cells expressing WT mo PrP (RKM 3), a highly expressive clone expressing WT mo PrP (RKM7), cells containing the empty vector (RKV), and RKM7 cells chronically infected with RML (RKM7/RML). Samples (50µg total protein) were run twice to confirm bands and probed with mAbs PRC5 at 1:5000 **(A)** and **(C)**, and GAPDH at 1:3000 **(B)** and **(D)**. No samples containing glycan substitutions showed detection of any PrP glycoforms or their derivatives. A transfer error resulted in band intensities representative of acceptably loaded samples as shown by GAPDH.

A

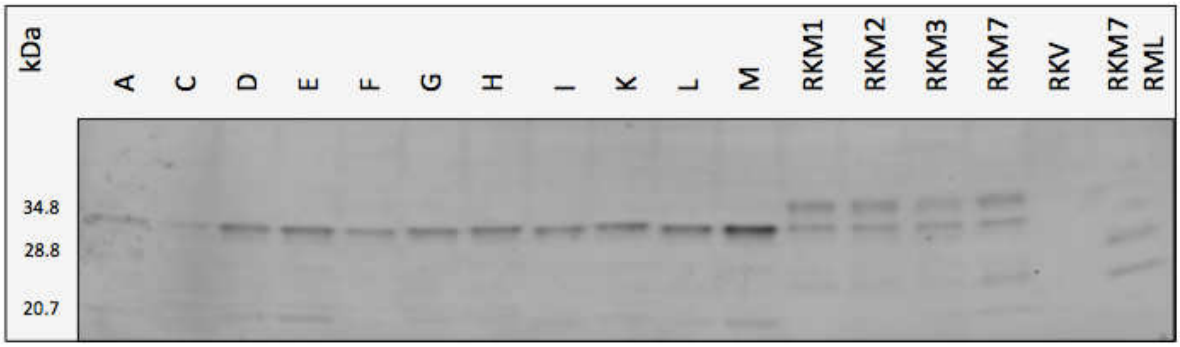

B

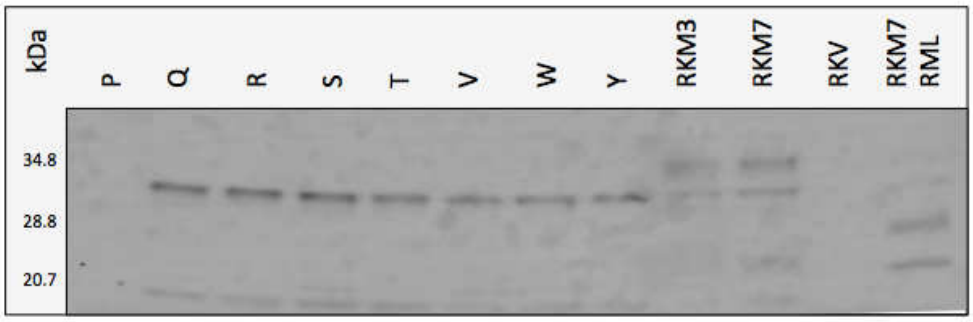

Figure 11. Representative N180 Site Mutation (Mono-1) Western Blots Probed with PRC7 N180 site mutations in mo PrP are shown along with controls including freshly infected cells expressing WT mo PrP (RKM 3), a highly expressive clone expressing WT mo PrP (RKM7), cells containing the empty vector (RKV), and RKM7 cells chronically infected with RML (RKM7/RML). Samples (50µg total protein) were run twice to confirm bands and probed with mAb PRC7 at 1:3000 **(A)** and **(B)**. All samples containing glycan substitutions with the exception of proline (P), showed detection of the PRC7-specific glycoform, aglycosylated full-length, and its derivative, C1. Blots were also probed with GAPDH to establish evenly loaded samples (data not shown).

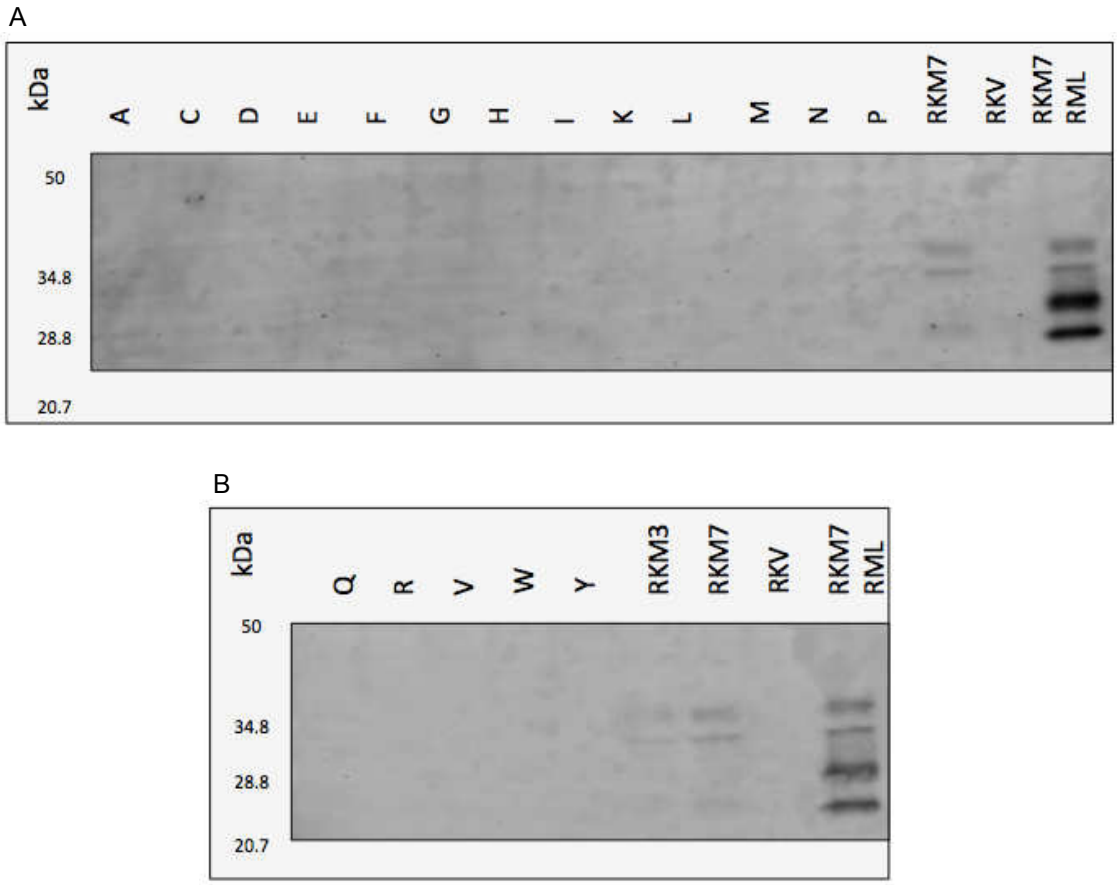

Figure 12. Representative S/T182 Site Mutation (Mono-1) Western Blots Probed with PRC7
S/T182 site mutations in mo PrP are shown along with controls including freshly infected cells expressing WT mo PrP (RKM 3), a highly expressive clone expressing WT mo PrP (RKM7), cells containing the empty vector (RKV), and RKM7 cells chronically infected with RML (RKM7/RML). Samples (50µg total protein) were run twice to confirm bands and probed with mAb PRC7 at 1:3000 **(A)** and **(B)**. No samples containing glycan substitutions showed detection of any PrP glycoforms or their derivatives. Blots were also probed with GAPDH to establish evenly loaded samples (data not shown).

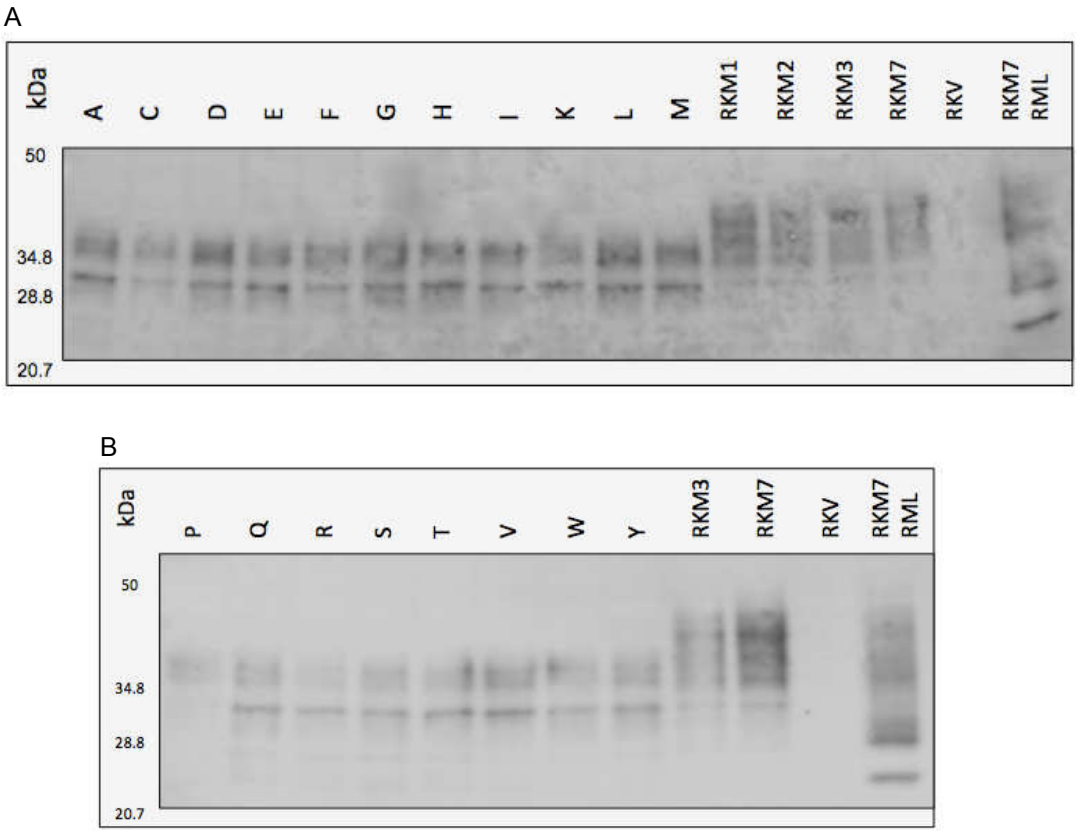

Figure 13. Representative N180 Site Mutation (Mono-1) Western Blots Probed with D13 N180 site mutations in mo PrP are shown along with controls including freshly infected cells expressing WT mo PrP (RKM 1-3), a highly expressive clone expressing WT mo PrP (RKM7), cells containing the empty vector (RKV), and RKM7 cells chronically infected with RML (RKM7/RML). Samples (50µg total protein) were run twice to confirm bands and probed with mAb D13 at 1:5000 **(A)** and **(B)**. All samples containing glycan substitutions with the exception of proline (P), showed detection of all PrP glycoforms, excluding the aglycosylated C1 derivative, as predicted, which is cleaved upstream of the D13 epitope. Blots were also probed with GAPDH to establish evenly loaded samples (data not shown).

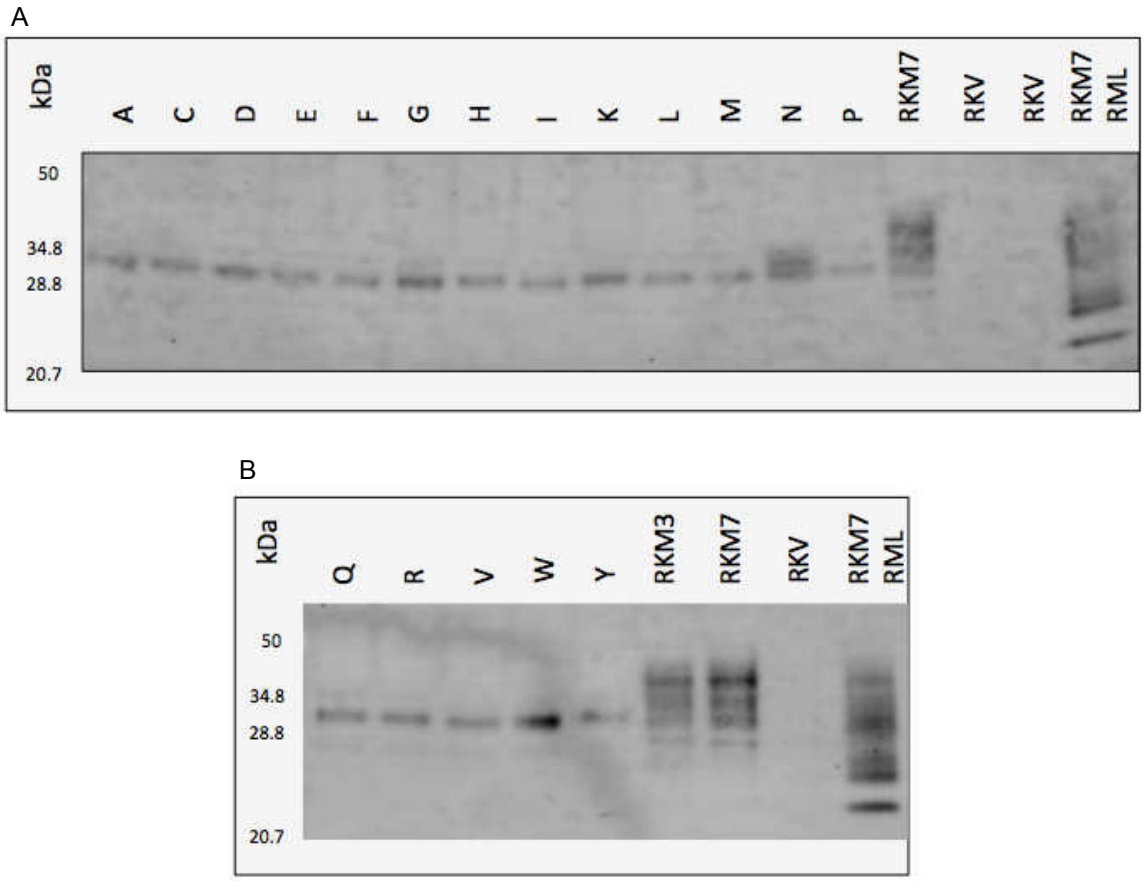

Figure 14. Representative S/T182 Site Mutation (Mono-1) Western Blots Probed with D13 S/T182 site mutations in mo PrP are shown along with controls including freshly infected cells expressing WT mo PrP (RKM 3), a highly expressive clone expressing WT mo PrP (RKM7), cells containing the empty vector (RKV), and RKM7 cells chronically infected with RML (RKM7/RML). Samples (50µg total protein) were run twice to confirm bands and probed with mAb D13 at 1:5000 **(A)** and **(B)**. All samples containing glycan substitutions showed detection of mono-2 full-length, with the exception of Asparagine (N), which shows mono-1 and mono-2 full-length due to the substitution of N for S/T. This substitution does not create a cryptic glycosylation site, as the downstream amino acid at 184 in the consensus sequence is lysine (K) not S or T. Blots were also probed with GAPDH to establish evenly loaded samples (data not shown).

Scrapie Cell Assay

The SCA developed previously by Klohn and colleagues has been utilized in our lab and modified for detection using newly developed mAbs (Bian et. al., 2010; Bian et. al., 2014). In this body of work, the SCA was used to determine which murine PrP N-glycan

substitutions play a significant role in prion propagation in RML, 22L, 139A, and mCWD prion isolates through single-cell PrP^{Sc} secretion.

Results from mutations made at sites N180 and S/T182 in murine PrP that were infected, plated, and analyzed through mAb D13 detection using SCA showed significant prion replication ($P \leq 0.001$) to near murine PrP control levels (RKM 1-3) as compared with RKV in the N180T mutant infected with RML, and in four 22L-treated N180 substitutions: N180D, N180E, N180K, and N180R (**Tables 1-2; Fig. 15**) when analyzed through one-way ANOVA with Tukey's multiple comparison test. These data suggest that N180 site mutations T, D, E, K, and R play a role in murine conversion of PrP^{C} to PrP^{Sc}. Additionally, these findings combined with preliminary data by Kang and colleagues further emphasize the importance of looking at individual amino acid changes at each of the two N-linked glycan sites on PrP to study their effects on propagation prior to further investigation in murine models.

The properties of the N180 substitutions that allowed prion propagation to occur are summarized in **Table 5**. The only commonality between these mutations is the physical property of polarity (**Table 5**). As glycosylation does not encompass everything influencing PrP conversion, it is also necessary to further examine the effects of polarity in prion disease highlighting the differences between polar mutations that allowed prion propagation and those that did not.

Alternatively, data show that there was a complete absence of prion propagation in all S/T182 mutant cells (**Tables 3-4; Fig. 16**). It can be postulated that there is no prion

propagation for mutations at the S/T182 site by SCA using mAb D13, yet one mono-2 full-length band is detected by immunoblotting because of the possibility that PrP is expressed at some level in the S/T182 mutations but may not be transported to the cellular surface to be able to become infected by prions. In other words, the proper cellular expression of PrP that is required for the conversion of PrP^{C} to PrP^{Sc} in the S/T182 mutants is not available, yet a partially processed form of PrP within the cytoplasm of the cell was available to be extracted and analyzed through western blot analysis as PrP^{C}. Moreover, after infection and subsequent PrP^{C} removal in the SCA, there was no protease resistant core available for detection with D13 in any S/T182 substitution.

Table 1. Summary of PrP^{Sc} production in different murine prion isolates for N180 site substitutions

	NBH			RML			22L			139A			mCWD		
A	10	7	6	135	68	82	36	53	58	22	8	40	21	18	14
C	10	12	4	70	30	56	17	9	9	25	12	14	16	15	10
D	6	13	3	130	77	54	1305	1079	1282	52	117	45	20	30	26
E	3	1	7	49	39	19	1105	1223	1297	17	15	10	45	12	8
F	6	5	11	45	37	48	35	19	29	15	14	12	18	15	17
G	6	4	4	33	25	13	25	26	12	12	8	12	13	13	15
H	10	9	17	94	56	41	26	24	20	14	5	7	13	18	23
I	4	12	8	72	121	128	16	26	23	23	18	18	11	16	15
K	4	7	10	49	56	65	814	905	1129	38	22	35	10	11	18
L	3	8	13	45	38	59	29	18	13	19	23	14	15	12	8
M	9	3	9	39	37	70	10	13	8	8	10	14	16	18	17
P	5	6	9	47	36	100	16	16	11	6	9	9	20	16	33
Q	6	6	13	73	44	46	111	107	68	4	4	11	9	17	24
R	3	17	18	45	51	20	401	658	593	14	14	12	10	14	32
S	2	11	12	130	73	96	35	16	41	20	27	64	17	18	-
T	7	11	7	298	213	237	12	11	11	17	10	11	17	14	19
V	21	7	13	99	70	32	29	23	19	14	19	52	9	14	12
W	3	4	10	60	36	55	13	4	-	11	17	14	24	13	18
Y	7	3	23	36	52	54	9	17	12	15	13	15	16	27	10
RKM1	12	6	2	225	509	259	1453	1158	894	380	310	196	68	175	212
RKM2	9	8	24	257	559	450	1293	1410	1196	496	552	640	190	181	282
RKM3	13	6	6	153	177	350	1119	1063	1180	211	330	74	132	73	113
RKM7	17	11	7	977	851	752	2267	1942	2090	803	1228	1107	960	793	597
RKV	13	9	6	36	34	32	15	9	14	11	17	13	26	25	23
RKM7/RML	1737	2036	1888	1641	1637	1888	1749	2086	2227	1688	2016	2120	1671	2334	-

Summary of individual cell spot counts per well representing PrP^{Sc} production in prion isolates RML, 22L, 139A, and mCWD and NBH for N180 mutation substitutions. Each mutation and control was infected in triplicate and plated onto ELISpot plates 4-weeks after infection. Prion replication was detected to near mo PrP control levels (RKM 1-3) in one mutant infected with RML (T), and in four 22L treated mutants (D,E,K, and R).

Table 2. Averages of PrP^{Sc} production in different murine prion isolates for N180 site substitutions

	Average	Average	Average	Average	Average
A	7.7	95.0	49.0	23.3	17.7
C	8.7	52.0	11.7	17.0	13.7
D	7.3	87.0	1222.0	71.3	25.3
E	3.7	35.7	1208.3	14.0	21.7
F	7.3	43.3	27.7	13.7	16.7
G	4.7	23.7	21.0	10.7	13.7
H	12.0	63.7	23.3	8.7	18.0
I	8.0	107.0	21.7	19.7	14.0
K	7.0	56.7	949.3	31.7	13.0
L	8.0	47.3	20.0	18.7	11.7
M	7.0	48.7	10.3	10.7	17.0
P	6.7	61.0	14.3	8.0	23.0
Q	8.3	54.3	95.3	6.3	16.7
R	12.7	38.7	550.7	13.3	18.7
S	8.3	99.7	30.7	37.0	17.5
T	8.3	249.3	11.3	12.7	16.7
V	13.7	67.0	23.7	28.3	11.7
W	5.7	50.3	8.5	14.0	18.3
Y	11.0	47.3	12.7	14.3	17.7
RKM1	6.7	331.0	1168.3	295.3	151.7
RKM2	13.7	422.0	1299.7	562.7	217.7
RKM3	8.3	226.7	1120.7	205.0	106.0
RKM7	11.7	860.0	2099.7	1046.0	783.3
RKV	9.3	34.0	12.7	13.7	24.7
RKM7/RML	1887.0	1722.0	2020.7	1941.3	2002.5

Averages of individual cell spot counts representing PrP^{Sc} production in prion isolates calculated from triplicate well numbers in **Table 1**.

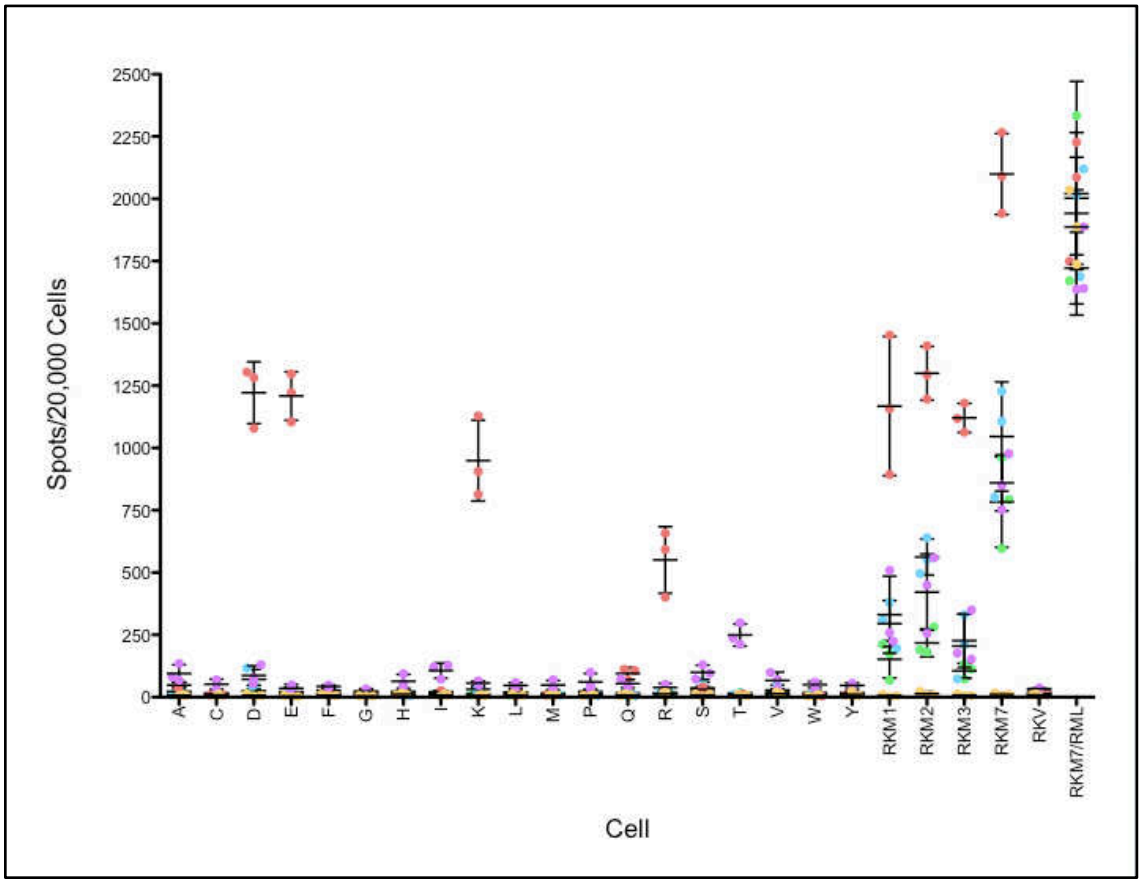

Figure 15. Scrapie Cell Assay N180 PrP^{Sc} production in different murine prion RML (purple), 22L (red), mCWD (green), and 139A (blue), as well as control NBH (orange) for the N180 site substitutions. Each mutation was infected and plated along with controls; freshly infected cells expressing WT mo PrP (RKM 1-3), a highly expressive clone expressing WT mo PrP (RKM7), cells containing the empty vector (RKV), and RKM7 cells chronically infected with RML (RKM7/RML), onto ELISpot plates 4-weeks after infection. Detection of infected cells was done using mAb D13 at 1:600. Prion replication was detected to near mo PrP control levels (RKM 1-3) in one mutant infected with RML (T), and in four 22L treated mutants (D, E, K, and R) as also shown in **Tables 1** and **2**.

Table 3. Summary of PrP^{Sc} production in different murine prion isolates for S/T182 site substitutions

	NBH			RML			22L			139A			mCWD		
A	9	14	7	29	8	13	9	4	8	24	22	22	9	14	5
C	8	11	8	14	11	12	23	6	17	14	8	12	5	6	7
D	6	3	5	12	9	14	9	19	12	11	10	22	12	6	5
E	9	4	8	27	8	3	22	18	11	34	9	15	9	6	11
F	4	4	8	35	6	10	6	4	7	19	8	12	5	1	6
G	1	11	1	17	17	15	19	13	13	17	10	15	13	24	9
H	4	6	9	18	17	11	21	15	13	12	17	17	21	12	18
I	21	6	11	16	14	20	25	14	31	20	15	19	14	23	11
K	9	13	7	12	22	24	15	11	15	14	11	-	5	10	10
L	5	5	8	11	12	11	7	9	9	45	9	12	11	6	4
M	7	2	5	10	12	23	14	17	7	14	11	6	4	3	5
N	16	5	7	15	7	13	7	14	27	10	19	11	4	8	6
P	2	14	6	6	10	16	12	12	22	26	12	16	6	14	10
Q	2	8	9	11	4	23	6	11	14	13	14	9	13	10	5
R	5	6	7	12	13	8	12	19	25	14	8	7	10	7	20
V	3	8	7	11	20	13	24	24	26	18	21	8	13	11	7
W	10	7	3	16	15	10	9	18	19	33	10	37	3	7	6
Y	12	5	5	17	21	11	15	14	20	18	32	15	4	11	4
RKM3	5	4	5	386	348	457	1191	883	867	247	496	221	85	55	74
RKM7	7	1	9	971	1022	955	1837	1452	1475	1121	885	850	614	844	600
RKV	5	7	9	26	20	23	23	14	28	10	17	11	34	40	20
RKM7/RML	1422	1612	1697	1950	1447	1340	2099	1941	2310	1689	1639	1640	1827	1855	2074

Summary of individual cell spot counts per well representing PrP^{Sc} production in prion isolates RML, 22L, 139A, and mCWD and NBH for S/T182 mutation substitutions. Each mutation and control was infected in triplicate and plated onto ELISpot plates 4-weeks after infection. Prion replication was not detected to near control mo PrP levels (RKM 3) in any prion isolate tested.

Table 4. Average of PrP^{Sc} production in different murine prion isolates for S/T182 site substitutions

	Average	Average	Average	Average	Average
A	10.0	16.7	7.0	22.7	9.3
C	9.0	12.3	15.3	11.3	6.0
D	4.7	11.7	13.3	14.3	7.7
E	7.0	12.7	17.0	19.3	8.7
F	5.3	17.0	5.7	13.0	4.0
G	4.3	16.3	15.0	14.0	15.3
H	6.3	15.3	16.3	15.3	17.0
I	12.7	16.7	23.3	18.0	16.0
K	9.7	19.3	13.7	12.5	8.3
L	6.0	11.3	8.3	22.0	7.0
M	4.7	15.0	12.7	10.3	4.0
N	9.3	11.7	16.0	13.3	6.0
P	7.3	10.7	15.3	18.0	10.0
Q	6.3	12.7	10.3	12.0	9.3
R	6.0	11.0	18.7	9.7	12.3
V	6.0	14.7	24.7	15.7	10.3
W	6.7	13.7	15.3	26.7	5.3
Y	7.3	16.3	16.3	21.7	6.3
RKM3	4.7	397.0	980.3	321.3	71.3
RKM7	5.7	982.7	1588.0	952.0	686.0
RKV	7.0	23.0	21.7	12.7	31.3
RKM7/RML	1577.0	1579.0	2116.7	1656.0	1918.7

Averages of individual cell spot counts representing PrP^{Sc} production in prion isolates calculated from triplicate well numbers in **Table 3.**

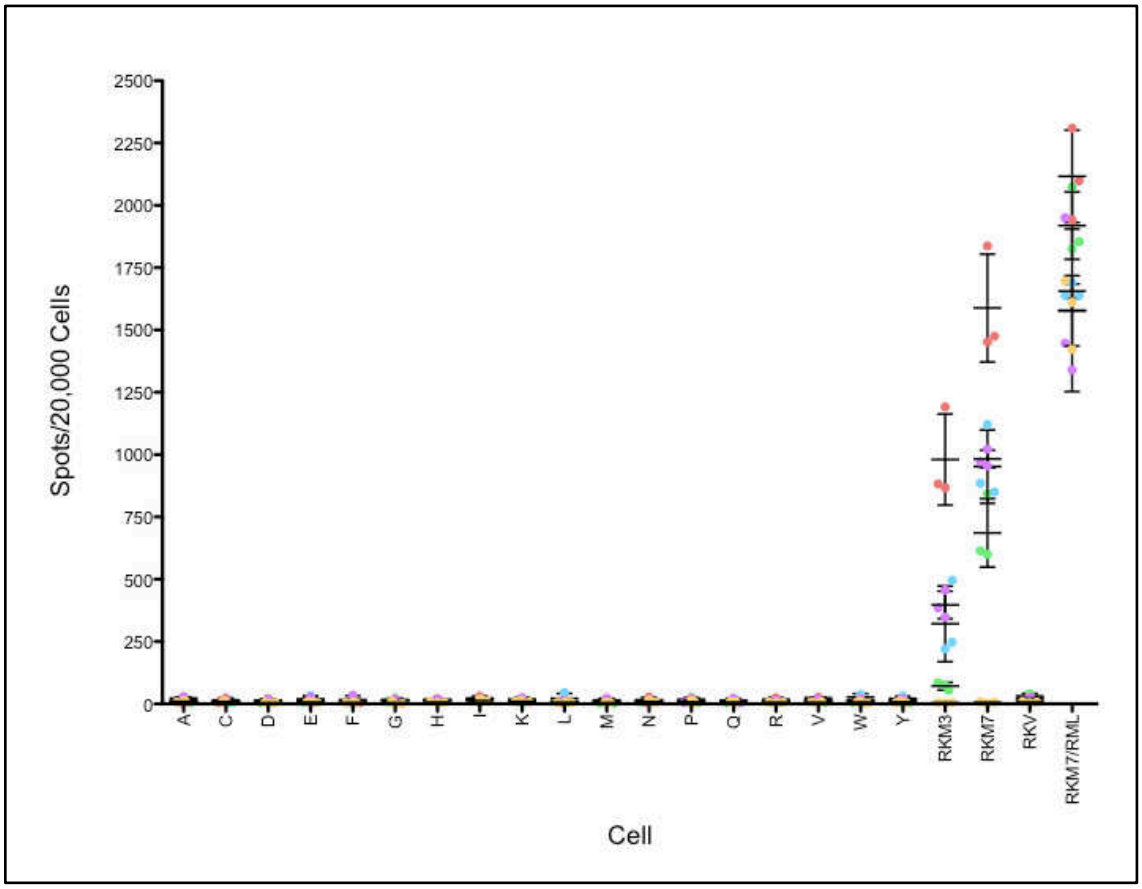

Figure 16. Scrapie Cell Assay S/T182 PrP^{Sc} production in different murine prion isolates RML (purple), 22L (red), mCWD (green), and 139A (blue), as well as control NBH (orange) for the S/T182 site substitutions. Each mutation was infected and plated along with controls; freshly infected cells expressing WT mo PrP (RKM 3), a highly expressive clone expressing WT mo PrP (RKM7), cells containing the empty vector (RKV), and RKM7 cells chronically infected with RML (RKM7/RML), onto ELISpot plates 4-weeks after infection. Detection of infected cells was done using mAb D13 at 1:600. Prion replication was not detected to near control mo PrP levels (RKM 3) in any prion isolate tested as also shown in **Tables 3** and **4**.

Table 5. Summary of the properties of amino acid substitutions at N180 that allowed successful prion replication

Name	Abbreviation	DNA Codon	Essential/ Non-Essential	Chemical Properties	Physical Properties
Threonine	T	ACT, ACC, **ACA**, ACG	Essential (diet)	Non-aromatic, hydroxylic	Polar (uncharged)
Aspartic Acid	D	GAT, **GAC**	Non-Essential (synthesized)	Acidic	Polar (negatively charged)
Glutamic Acid	E	**GAA**, GAG	Non-Essential (synthesized)	Acidic	Polar (negatively charged)
Lysine	K	**AAA**, AAG	Essential (diet)	Basic	Polar (positively charged)
Arginine	R	CGT, CGC, CGA, CGG, **AGA**, AGG	Non-Essential (synthesized)	Basic	Polar (positively charged)

Summary of N180 substitutions that showed a significant increase ($P \leq 0.001$) in prion replication to near WT levels (RKM 1-3) in one mutant infected with RML (T), and in four 22L treated mutants (D,E,K, and R). Bolded codons were used in the generation of these constructs. The one consistent similarity between all of these substitutions is the physical property of polar charge.

Genetic Sequencing

Finally, in terms of the outcomes of PCR amplification and subsequent DNA sequencing of three constructs, S/T182W (tryptophan), S/T182Y (tyrosine), and N180D (aspartic acid), the successful generation of stable RK13 cells expressing mutations at either N180 or S/T182 on murine PrP was confirmed (**Figs. 17; 18**). All samples showed positive bands for murine puro PrP (~820bp) and CMV (~351bp), indicating the presence of these sequences in the DNA of the stably transfected cells. Additionally, DNA sequencing results confirmed the correct mutation for each construct in murine

PrP. One thing of importance to note is that the N180D construct is one of four that showed significant prion propagation in 22L while S/T182W and Y are constructs that did not allow prion proliferation. Therefore, the lack of prion replication in the S/T182 mutations cannot be explained by the absence of the correct inserts incorporated into the gene.

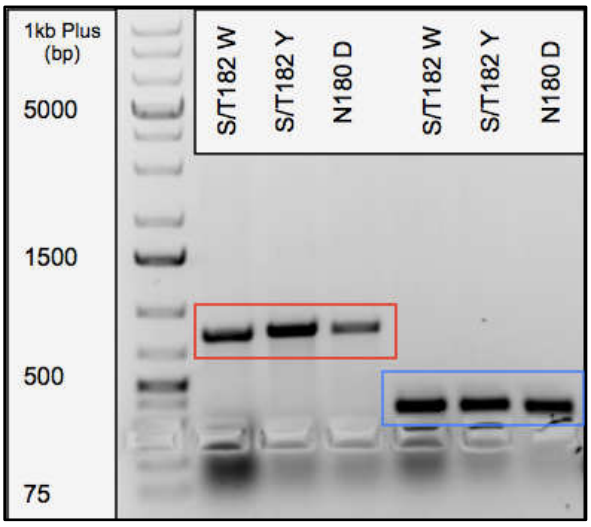

Figure 17. Murine PrP and CMV PCR Agarose gel of amplified 500ng of DNA template from three representative N180 and S/T182 site mutations. Mo puro PrP (red box), CMV promoter (blue box). Two representative S/T182 substitutions negative for prion propagation and one N180 mutation shown to replicate prions were chosen for PCR amplification and genetic sequencing to confirm stable transfections. All samples showed positive bands for mo puro PrP (~820bp) and CMV (~351bp), suggesting the proper insertion of these sequences in the DNA of the stably transfected RK13 cells.

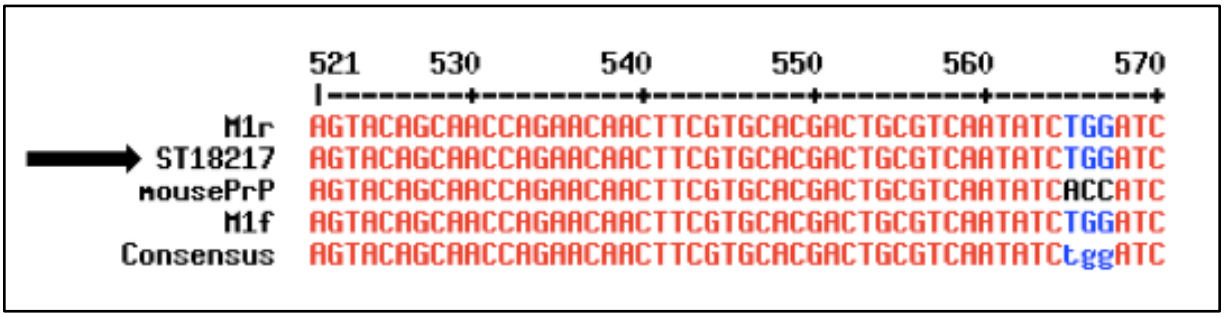

Figure 18. Murine PrP DNA Sequencing Analysis of one representative mutant PrP DNA shows the confirmation of the correct PrP sequence for the S/T182W mutation (arrow) as compared with mo WT PrP. No other alterations in the PrP sequence was detected in any of the three constructs examined.

Discussion

In recent years, more work has been implemented into improving our understanding of the role of glycosylation in prion disease (Cancellotti et. al., 2005; Cancellotti et. al., 2010; DeArmond et. al., 1997; Tuzi et. al., 2008). Preliminary data by Kang and colleagues combined with the results in this body of work collectively show the first evidence of the effects of underglycosylation on prion prorogation by treating each N-glycan attachment site on PrP individually.

In this body of work, individual amino acid substitutions were made at two points on the mono-1 glycan attachment encompassing the consensus sequence NXS/T. Removal of this glycosylation event permitted the study of the role of underglycosylation in prion disease. This approach to the current study was largely based on unpublished data obtained by Kang and colleagues in which the mono-2 N-glycan site on murine PrP was individually mutated at either N196 or T198 to each of the remaining 19 amino acids. Afterward, cells were treated with NBH, and prion isolates RML, 22L, 139A, and mCWD and analyzed for prion propagation.

Ablation of the Mono-1 N-Glycan Attachment on PrP and PrP^C expression

Western blots have traditionally been used as a reliable readout to detect prion disease (Hadlow, 1999; Hnasko et. al., 2010; MacGregor, 2001; Pawel, 2004). In this body of work, we analyzed immunoreactive bands for N-glycan mutations made at N180 and S/T182 of murine PrP. PrP^C expression was visualized using mAbs PRC5, PRC7, and D13. Results confirmed the ablation of the mono-1 N-glycan attachment at both sites.

All N180 site mutations exhibited the expected PrP glycoforms and their derivatives with the exception of P when probed with mAbs PRC5, PRC7, and D13. It has been demonstrated that P cannot be located in the second motif of the consensus sequence, NXS/T. This is largely due to the fact that P is bound in a loop that forms a 180-degree turn. Therefore, it can be assumed that the substitution at N180P acts in a similar way (Marshall, 1972). Additionally, N180 glycan results confirm that the lack of one glycan attachment in the mutants does not de-stabilize the entire protein structure to the extent where they acquire PrP^{Sc} like characteristics, such as a protease resistant core (Lehmann and Harris, 1997; Korth et. al., 2000; Winklhofer et.al., 2003). However, it was shown that PrP with alterations to N-glycans exhibit evidence of PrP^{Sc} like characteristics, like insolubility in detergents, while maintaining sensitivity to protease treatment (Neuendorf et. al., 2004).

Interestingly, results from western blot analysis of substitutions made at S/T182 on murine PrP resulted in the complete absence of immunodetection with conformationally dependent mAbs PRC5 and PRC7. When probed with D13, a mAb located in the

unstructured region consisting of a linear epitope, one lower immunoreactive band for mono-2 full-length was detected in all mutations with the exception of S/T182N, in which a doublet formed resembling the banding pattern of the N180 substitutions stained with D13. Overall, these results suggest that PrP is expressed to some level in the S/T182 mutations, but may not be transported to the cellular surface for detection or prion conversion. Moreover, the primary sequence for the N-glycan substitution S/T182N was checked at amino acid 184 to confirm that a new cryptic glycosylation site was not initiated.

Ablation of the Mono-1 N-Glycan Attachment on PrP and Prion Propagation

Prior attempts have been made to address the role of post-translational modifications in prion propagation. However, these studies fail to recognize prion biology in its entirety. Any mutation at the first or the third amino acid of the glycan consensus sequence on PrP results in the ablation of glycan attachment. Therefore, it is necessary to study point mutation changes at each of the two N-linked glycan sites on PrP and analyze their effects on propagation prior to investigation at the level of the organism.

Earlier investigations include *in-vivo* PrP glycosylation studies using knock-in or gene replacement approach to partly or fully ablate glycan attachments on PrP in mice that substitute T for N. These studies have reported little to no prion propagation (Cancellotti et. al., 2005; Cancellotti et. al., 2010). Importantly, these substitutions have been described to affect PrP processing through the secretory pathway, and make it difficult to determine whether the lack of transmissibility of PrP^{Sc} might be related to

aglycosylation, potentially low concentrations of PrP^{C} on the cell surface, or improper folding of the tertiary structure (Capellari at. al., 2000; Korth et. al., 2000).

Other research include studies completed by DeArmond and colleagues in which genetically modified mice were generated with an A replacing the T at each N-glycan site. Results indicated that prion transmission to these mice was strain-selective and less efficient than in mice expressing normal PrP glycosylation (DeArmond et. al., 1997; Tuzi et. al., 2008). Therefore, it is uncertain whether or not these discrepancies might be related to the varying amino acid substitutions used to obliterate PrP glycosylation.

In the present study, the SCA was chosen as the main readout for prion propagation and used prion strains RML, 22L, 139A mCWD, and NBH control. This assay was selected based off of its highly immune-sensitive properties to measure the number of PrP^{Sc} secreting cells post-infection. Immunodetection of experimentally infected RKM, RKV, RKM7, and RK13 glycan point mutations were performed using mAb D13 as described formerly (Bian et. al., 2010; Bian et. al., 2014). Data obtained from mutations made at N180 and S/T182 encompassing the mono-1 glycan site showed significant prion propagation ($P \leq 0.001$) equivalent to RKM control levels after infection with RML or 22L in N180T, N180D, N180E, N180K, and N180R. These data suggest that N180 site mutations T, D, E, K, and R play a role in murine conversion of PrP^{C} to PrP^{Sc}. Alternatively, a complete absence of prion replication was found in all modifications made at S/T182 with each strain tested. These results may indicate a lack of

membrane-bound PrP^{C} that is necessary for conversion likely caused by a disruption in cellular processing and trafficking.

One potential flaw in the results of the SCA of this study is that only the RKM7 WT control samples infected with prion strain 22L exhibited PrP^{Sc} positive cell numbers comparable to the chronically infected control, RKM7/RML. This outcome makes the data inconclusive without additional replicates. It is possible that these results may be due to either a technical error in the assay, or to a BH titer difference that was not accounted for. Brain weight does not necessarily correspond with the amount of PrP^{Sc} in a sample. Therefore, it can be assumed that there was likely some variability in PrP^{Sc} expression between BHs used in this study. To account for this, replicate studies should be performed using several isolates for each strain and a consistent trend observed before results can be considered conclusive.

In contrast to the aforementioned study performed by Cancellotti and colleagues, our N180T mutation at mono-1 resulted in the detection of significant levels of PrP^{Sc} by SCA after infection with RML to near RKM levels (Cancellotti et. al., 2005; Cancellotti et. al., 2010). Furthermore, preliminary data by Kang and colleagues demonstrated that the N196T mutation at mono-2 had an increase in the levels of PrP^{Sc} by SCA when infected with RML, 22L, 193A, and mCWD. Therefore, the substitution of T for N at either glycan site on PrP may play a role in prion replication. Alternatively, in the present study, there was a complete absence of prion propagation in all substitutions made at the third sequon S/T182 of the consensus sequence at mono-1 when infected with RML, 22L,

139A, and mCWD. These results may bring insight into why lower replication efficiency was seen in genetically modified mice consisting of an A rather than a T at each glycan site on PrP as seen in former investigations by DeArmond and colleagues (DeArmond et. al., 1997).

Ablation of the Mono-1 N-Glycan Attachment on PrP and Trafficking to the Cell Membrane

As previously thought, complete sugar attachment is not required to make a glycoprotein functional and stable (Heleius and Aebi, 2001; Lowe and Marth, 2003). In 2005, it was shown by Cancellotti and colleagues that the presence of a single sugar chain is adequate enough for the successful trafficking of PrP to the cell membrane (Cancellotti et. al., 2005). They also reported that while glycans appear to control the cellular location of PrP, the presence of sugars does not considerably change its biology. In the present study, we addressed the same question using our point mutation *in-vitro* model of N-glycosylation by altering each of the sugar attachments on PrP to each of the remaining amino acids and treating them individually.

In the current study, mutations were made at mono-1 at two locations and contain only one N-glycan attachment at mono-2. These alterations do not create an immature glycoprotein unable to be expressed at the cell surface as suggested (Hershko and Ciechanover, 1998; Neuendorf et. al., 2004; Petersen et. al., 1996). These inferences are supported by successful PrP^{C} immunodetection in the N196, T198, and N180 site substitutions by conformationally dependent mAbs that require discontinuous epitopes.

Moreover, after infection, mutations N180T, N180D, N180E, N180K, N196K, and N180R resulted in significant and quantifiable PrP^{Sc} expression that is comparable to RKM levels by SCA. This further suggests that these mutations were processed correctly in the cell despite the lack of one glycan attachment.

However, the substitutions made at the S/T182 site are an exception to these conclusions. In general, the inability for these mutations to express immunoreactive bands using conformationally dependent mAbs that are consistent with expected PrP glycoforms indicates that they were not fully processed and anchored at the cell surface. One explanation for this outcome is that the because mono-1 is located directly in α-helix 2, the S/T182 point mutations disrupt the three-dimensional structures of PrP to the extent that the un-manipulated mono-2 N-glycan attachment is unable to become fully glycosylated as shown by immunoreactive bands for the N180 mutations. This outcome may be due to possible steric hindrance of the folding of the protein. As a consequence, all S/T182 mutations, with the exception of S/T182N, may have resulted in a species of PrP that does not have a fully glycosylated glycan at mono-2 as demonstrated by the difference in band width when comparing D13 blots between the S/T182 and N180 site mutants. Therefore, the point mutations made at S/T182 may represent more of an aglycosylated species of PrP. This theory is supported by research that shows aglycosylated PrP gets trapped intracellularly during processing (DeArmond et. al., 1997; Lehmann and Harris, 1997; Harris, 2003; Rogers et. al., 1990). Alternatively, Korth, Neuendorf, and colleagues were able to detect aglycosylated PrP at the cell surface of cells containing several N-glycan mutants. Regardless, these data

suggest that the modification of a single amino acid, rather than the complete absence of a sugar attachment can influence cellular localization of PrP (Korth et. al., 2000; Neuendorf et. al., 2004).

Ablation of the Mono-1 N-Glycan Attachment on PrP and Secondary and Tertiary Structures

Of the 20 amino acids that occur naturally, 6 are considered to be clearly polar. These include negatively charged D and E, positively charged R, and K, as well as uncharged N and Q (Betts and Russell, 2003). Other slightly polar or indifferent amino acids include H, A, Y, T, S, P and G. The properties of the amino acid are due to the side-chain group (R-group) which is important when it comes to the primary structure of a protein. These properties drive the folding and intrarmolecular bonding of the linear amino acid chain that determines the protein's overall shape. All polar amino acids have a hydrophilic side-chain when in an aqueous environment and can therefore make hydrogen bonds with other suitable groups. For this reason, these amino acids are found exposed on the surface of a protein (Betts and Russell, 2003).

Due to the nature of the weak interactions controlling the three dimensional structure, proteins are very sensitive molecules. The native state can be disrupted by a number of external stress factors including pH or the removal of water (Betts and Russell, 2003) Moreover, any mutation that causes an amino acid substitution can have a large influence on protein structure and subsequent protein function. In this body of work, only strongly polar amino acid substitutions, N180D, N180E, N180K, and N180R, resulted in

prion propagation with the exception of one slightly polar replacement, N180T through detection by SCA. The chemistry of amino acid side chains is critical to protein structure because they bond with one another and hold the protein in a certain conformation. Regardless, the alterations of the primary sequence on murine PrP made at mono-1 that allow prion replication share the property of polarity with the native amino acid N at residue 180 in PrP. This common characteristic could mean that a polar amino acid at residue 180 of mono-1 is required for the successful conversion of PrP^{C} to PrP^{Sc} by maintaining the α-helix structure. This finding is novel because mono-1 resides within the second helix of PrP and any change in primary structure can greatly impact subsequent protein folding and interactions.

It is important to point out that not every polar mutation made in this study supported prion propagation. Furthermore there was no consistency observed between the charge of the side-chain and prion conversion. These realizations result in further questions regarding point mutation changes at the N-glycan consensus sequence and their involvement in prion propagation. It is no surprise then that generating and assessing individual amino acid mutations for each of the N-glycan sites on PrP was both time consuming and costly. There are other ways in which investigators could strategically manipulate the consensus sequence and ask a more specific question. However, this body of work lays important groundwork that provides an overview for other researchers to base new questions on in future investigations.

It remains uncertain whether or not an intermediate species of PrP is required for conversion of PrP^{C} to PrP^{Sc}. Solving the structure of PrP^{C} has provided one part of the equation, however our lack of knowledge of the tertiary structure of PrP^{Sc} remains a clear deficiency. An emphasis needs to continue on studying the post-translational differences between PrP^{C} and PrP^{Sc} in order to fully understand the prion hypothesis and PrP^{Sc}. Deciphering the structure of PrP^{Sc} will then identify how PrP^{C} is altered and lead to a better understanding of the mechanism of conversion and succeeding treatment and prevention of prion disease.

CHAPTER 3 – CONCLUSIONS AND FUTURE DIRECTIONS

Conclusions

This body of work completes the initial series of studies started by Kang and colleagues to decipher the role of aglycosylation in prion disease through amino acid substitutions at each of the two N-glycan sites on murine PrP and subsequent prion conversion using four prion strain isolates (RML, 22L, 139A and mCWD).

Collectively, these studies show the first evidence of the effects of aglycosylation on prion propagation by treating each of the glycan attachment sites on PrP individually. These preliminary findings establish the importance of post-translational differences between PrP^{C} and PrP^{Sc} which constitute an essential, unresolved aspect of the prion hypothesis several decades after it was first proposed. The core hypothesis of this body of work, that PrP^{Sc} is preferentially generated during prion propagation, in addition to the specific aims addressed which attempt to investigate the relationship of individual mono-1 mutations on murine PrP through PrP^{C} expression and subsequent propagation using four prion isolates, represent both a novel and significant development in understanding the mechanism by which prions replicate.

Future Directions

Processing of PrP Mutants

Once preliminary results from this body of work are confirmed through additional experimental replications, further investigations will be performed to examine the

processing of these N-linked glycan mutations in the cell prior to infection. These experiments will include assays in which the trafficking, distribution, and cellular membrane occupancy of the individually mutated prion proteins can be studied. While the proper folding of PrP in combination with the ability to support prion propagation is consistent with correct protein processing and cellular distribution, it is important to confirm, especially in S/T182 mutants in which prion propagation was entirely un-detected, that the mutated proteins at both mono-1 and mono-2 were able to reach the cellular membrane successfully. These studies could be executed by using genetically encoded fluorophores, such as super ecliptic pHluorin (SEP), a PH-sensitive derivative of green fluorescent protein (GFP) commonly used in live cell imaging (Ashby et. al., 2004; Sankaranarayanan et. al., 2000) In these experiments, SEP would be used as a tag to visualize PrP within living cells in real-time. These studies will allow us to determine whether or not the S/T182 site mutations specifically are being processed correctly or getting stuck in the cell resulting in the inability for them to be expressed at the cell surface. Alternatively, immunocytochemical prion detection using discriminatory and non-discriminatory mAbs followed by flow cytometry would be another means to differentiate between mutants that were successfully processed and mutants that were not.

Biochemical Analysis

Following the confirmation of proper processing within the cell, biochemical analysis of cells containing each mutated PrP will be performed. In these experiments, fractionation techniques would be used to separate various cellular components such as organelles

and macromolecules. Fractionation would allow us to reduce the size of the protein pool to be analyzed and enable us to focus on proteins located within certain cellular compartments. This would enable us to focus specifically on PrP for analysis and interpretation so we can characterize the PrP mutations with respect to mono-1 or mono-2.

Other Future Studies

Coupled with NMR or x-ray crystallography, these techniques would allow us to obtain functional and structural information regarding these N-glycan substitutions in PrP. Our goal would be to introduce mutations at both the mono-1 and mono-2 sites on PrP into RK13 cells that consist solely of the formation of aglycosylated murine PrP with the capability for prion conversion. These cells would undergo infection using several prion isolates and control NBH. Thereafter, the same analyses would be performed on these double mutants with potential to move forward to *in-vivo* mouse models for further evaluation at the level of the organism.

REFERENCES

Alberts B, Johnson A, Lewis J, et. al. 2002. *Analyzing protein structure and function*. Molecular Biology of the Cell, 4th edition New York: Garland Science.

Alberts B, Johnson A, Lewis J, et. al. 2002. *Fractionation of cells*. Molecular Biology of the Cell, 4th edition New York: Garland Science.

Alper T, Haig DA, Clarke MC. 1966. *The exceptionally small size of the scrapie agent.* Biochem. Biophys. Res. Commun. 22:278-84.

Alper, T, Cramp WA, Haig DA, Clarke MC. 1967. *Does the agent of scrapie replicate without nucleic acid?* Nature 214:764-66.

Alpers MP, Prusiner SB, McKinley MP. 1987. *Epidemiology and clinical aspects of kuru, Prions: Novel infectious pathogens causing scrapie and Creutzfeldt-Jakob disease*. San Diego Acad. Press 451-65.

Anderson RM, Donnelly CA, Ferguson NM, Woolhouse ME, Watt CJ, et. al.1996. *Transmission dynamics and epidemiology of BSE in British cattle*. Nature 382:779-88.

Angers RC, Kang HE, Napier D, Browning S, Seward T, et. al. 2010. *Prion strain mutation determined by prion protein conformational compatibility and primary structure*. Science 328:1154-58.

Ashby MC, Ibaraki K, Henley JM. 2004. *It's green outside: tracking cell surface proteins with pH-sensitive GFP*. Trends Neurosci. 27:257-61.

Barry RA, McKinley MP, Bendheim PE, Lewis GK, DeArmond SJ, Prusiner SB. 1985. *Antibodies to the scrapie protein decorate prion rods*. J. Immunol. 135:603-13.

Benestad S, Mitchell G, Simmons M, Ytrehus B, Vikoren T. 2016. *First case of chronic wasting disease in Europe in a Norwegian free-ranging deer*. Vet. Res. 47, 88.

Bessen RA, Marsh RF. 1992. *Identification of two biologically distinct strains of transmissible mink encephalopathy in hamsters*. J. Gen. Virol. 73:329-34.

Betts MJ, Russell RB. 2003. *Amino acid properties and consequences of substitutions.* Bioinformatics for Geneticists, Wiley: M.R. Barnes, I.C. Gray eds.

Bian J, Napier D, Khaychuck V, Angers R, Graham C, Telling G. 2010. *Cell-based quantification of chronic wasting disease prions*. J. Virol. 84:8322-26.

Bian J, Kang, HE, Telling GC. 2014. *Quinacrine promotes replication and conformational mutation of chronic wasting disease prions*. PNAS 111:6028-33.

Bolton DC, McKinley MP, Prusiner SB. 1982. *Identification of a protein that purifies with the scrapie prion*. Science 218:1309-11.

Bolton DC, Meyer RK, Prusiner SB. 1985. *Scrapie PrP 27-30 is a sialoglycoprotein*. J. Virol. 53:596-606.

Borchelt DR, Scott M, Taraboulos A, Stahl N, Prusiner SB. 1990. *Scrapie and cellular prion proteins differ in their kinetics of synthesis and topology in cultured cells*. J. Cell Biol. 110:743-52.

Bruce ME, Dickson AG. 1987. *Biological evidence that scrapie agent has an independent genome*. J. Gen. Virol. 68:79-89.

Bruce ME, McConnell I, Fraser H, Dickinson AG. 1991. *The disease characteristics of different strains of scrapie in Sinc congenic mouse lines: implications for the*

nature of the agent and host control of pathogenesis. J. Gen. Virol. 72:595-603.
Cancellotti E, Wiseman F, Tuzi NL, Baybutt H, Monaghan P et. al. 2005. *Altered glycosylated PrP proteins can have different neuronal trafficking in brain but do not acquire scrapie-like properties*. J. Biol. Chem. 280:42909-18.
Cancellotti, E, Barron RM, Bishop MT, Hart P, Wiseman F, Manson JC. 2007. *The role of host PrP in transmissible spongiform encephalopathies*. Biochim. Biophys. Acta. 1772:673-80.
Cancellotti, E, Bradford BM, Tuzi NL, Hickery RD, Brown D et. al. 2010. *Glycosylation of PrP^C determines timing of neuroinvasion and targeting in the brain following transmissible spongiform encephalopathy infection by a peripheral route*. J. Virol. 84:3464-75.
Capellari, S, Zaidi SI, Long AC, Kwon EE, Peterson RB. 2000. *The Thr183Ala mutation, not the loss of the first glycosylation site, alters the physical properties of the prion protein*. J. Alzheimers Dis. 2:27-35.
Caughey B, Raymond GJ. 1991. *The scrapie-associated form of PrP is made from a cell surface precursor that is both protease- and phospholipase-sensitive*. J. Biol. Chem. 266:18217-23.
Chen SG, Teplow DB, Parchi P, Teller JK, Gambetti P, Autiliogambetti L. 1995. *Truncated forms of the human prion protein in normal brain and in prion diseases.* J. Biol. Chem. 270:19173-80.
Cherng JY, Schuurmans-Nieuwenbroek NM, Jiskoot W, Talsma H, Zuidam NJ, et. al. 1999. *Effect of DNA topology on the transfection efficiency of poly((2-dimethylamino)ethyl methacrylate)-plasmid complexes*. J. Control Release. 60:343-53.
Cohen FE, Prusiner SB. 1999. *Prion Biology and Diseases*. Cold Spring Harbor Lab. Press 191-228.
Collinge J. 1997. *Human prion diseases and bovine spongiform encephalopathy (BSE)*. Hum. Mol. Genet. 6:1699-1705.
Collinge J. 1999. *Variant Creutzfeldt-Jakob disease.* Lancet 354:317-23.
Collinge J. 2001. *Prion diseases of humans and animals: Their causes and molecular basis*. Annual Reviews 24:519–50.
Cousens SN, Vynnycky E, Zeidler M, Will RG, Smith PG. 1997. *Predicting the CJD epidemic in humans*. Nature 385:197-98.
Cuille J, Chelle PL. 1936. *La maladie dite tremblante du mouton est-elle inocuable?* C. R. Acad. Sci. 203:1552-54.
DeArmond SJ, Sanchez H, Yehiely F, Qui Y, Ninchak-Casey A, et. al., 1997. *Selective neuronal targeting in prion disease*. Neuron 19:1337-48.
Dickson AG, Meikle VMH, Fraser H. 1968. *Identification of a gene which controls the incubation period of some strains of scrapie agent in mice*. J. Comp. Pathol. 78:293-99.
Dickson AG, Bruce ME, Outram GW, Kimberlin RH. 1984. *Proceedings of workshop on slow transmissible diseases*. Tateishi, J., Ed. 5-118, Japanese Ministry of Health and Welfare, Tokyo.
Dodelet VC, Cashman NR. 1998. *Prion protein expression in human leukocyte differentiation*. Blood Journal 1556-61.
Ford MJ, Burton LJ, Li H, Graham CH, Frobert Y, et. al. 2002. *A marked disparity*

between the expression of prion protein and its message by neurones of the CNS. Neuroscience 111:533-51.
Gajdusek DC, Gibbs CJ, Alpers MP. 1966. *Experimental transmission of a kuru-like syndrome to chimpanzees*. Nature 209:794-96.
Ghani AC, Ferguson NM, Donnelly CA, Hagenaars TJ, Anderson RM. 1998. *Epidemiological determinants of the pattern and magnitude of the vCJD epidemic in Great Britain*. Proc. Biol. Sci. 265:2443-52.
Gibbs CJ, Gajdusek DC, Asher DM, Alpers MP, Beck E, et. al. 1968. *Creutzfeldt-Jakob disease (spongiform encephalopathy): transmission to the chimpanzee*. Science 161:388-89.
Griffith JS. 1967. *Self replication and scrapie*. Nature 215:1043-44.
Gruffydd-Jones TJ, Galloway PE, Pearson GR. 1992. *Feline spongiform encephalopathy*. J. Small Anim. Pract. 33:471-76.
Hadlow WJ. 1959. *Scrapie and kuru*. Lancet 2:289-90.
Hadlow WJ. 1999. *Reflections on the transmissible spongiform encephalopathies*. Vet. Path. 529:523-29.
Halliday M, Radford H, Mallucci GR. 2014. Prions: *Generation and spread versus neurotoxicity*. J. Biol. Chem. 289:19862-68.
Hanson SR, Culyba EK, Hsu TL, Wong CH, Kelly JW, Powers ET. 2009. *The core trisaccharide of an N-linked glycoprotein intrinsically accelerates folding and enhances stability*. Proc. Natl. Acad. Sci. USA 106:3131-36.
Harris DA. 2003. *Trafficking, turnover and membrane topology of PrP*. Br. Med. Bull. 66:71-85.
Harstough GR, Burger D. 1965. *Encephalopathy of mink. 1. Epizootiologic and clinical observations*. J. Infec. Dis. 115:387-92.
Helenius A, Aebi M. 2001. *Intracellular functions of N-linked glycans*. Science 291:2364-69.
Hershko A, Ciechanover,A. 1998. *The ubiquitin system*. Annu. Rev. Biochem. 67:425-79.
Hill AF, Desbruslais M, Joiner S, Sidle KCL, Gowland I, et. al. 1997. *The prion strain causes vCJD and BSE*. Nature 389:448-50.
Hosszu LLP, Baxter NJ, Jackson GS, Power A, Clarke AR, et. al. 1999. *Structural mobility of the human prion protein probed by backbone hydrogen exchange*. Nat. Struct. Biol. 6:740-43.
Hnasko R, Serban AV, Carlson G, Prusiner SB, Stanker LH. 2010. *Generation of antisera to purified prions in lipid rafts*. Prion 4:94-104.
James TL, Liu H, Ulyanov NB, Farr-Jones S, Zhang H, et. al. 1997. *Solution structure of a 142-residue recombinant prion protein corresponding to the infectious fragment of the scrapie isoform*. Proc. Natl. Acad. Sci. USA 94:10086-91.
Kang HE, Weng CC, Saijo E, Saylor V, Bian J, et. al. 2012. *Characterization of conformation-dependent prion protein epitopes*. J. Biol. Chem. 287:37219-32.
Kellings K, Meyer N, Mirenda C, Prusiner SB, Riesner D. 1992. *Further analysis of nucleic acids in purified scrapie prion preparations by improved return refocusing gel electrophoresis*. J. Gen. Virol. 73:1025-29.
Klohn PC, Stoltze L, Flechsig E, Enari M, Weissmann C. 2003. *A quantitative, highly sensitive cell-based infectivity assay for mouse scrapie prions*. Proc. Natl. Acad.

Sci. USA.100:11666-71.
Korth C, Stierli B, Streit P, Moser M, Schaller O, et. al. 1997. *Prion (PrP^{Sc})-specific epitope defined by a monoclonal antibody*. Nature 390:74-7.
Korth C, Kaneko K, Prusiner SB. 2000. *Expression of unglycosylated mutated prion protein facilitates PrP(Sc) formation in neuroblastoma cells infected with different prion strains*. J Gen. Virol. 10:2555-63.
Kovacs GG, Makarava N, Savtchenko R, Baskakov IV. 2013. *Atypical and classical forms of the disease-associated state of the prion protein exhibit distinct neuronal tropism, deposition patterns, and lesion profiles*. Am. J. Path. 183:1539-47.
Kubler E, Oesch B, Paeber AJ. 2003. *Diagnosis of prion diseases*. BR. Med. Bull. 66:267-79.
Lawson VA, Collins SJ, Masters CL. 2005. *Prion protein glycosylation*. J. Neurochem. 93:769-1056.
Lehmann S, Harris DA. 1997. *Blockade of glycosylation promotes acquisition of scrapie-like properties by the prion protein in cultured cells*. J. Biol. Chem. 272:21479-87.
Lowe JB, Marth, JD. 2003. *A genetic approach to mammalian glycan function*. Annu. Rev. Biochem. 72:643-91.
MacGregor I. 2001. *Prion protein and developments in its detection*. TOC 11:3-14.
Marsh RF, Bessen RA, Lehmann S, Hartsough GR. 1991. *Epidemiological and experimental studies on a new incident of transmissible mink encephalopathy*. J. Gen. Virol. 72:589-94.
Marsh RF, Hadlow WJ. 1992. *Transmissible mink encephalopathy*. Rev. Sci. Tech. 11:539-50.
Marshall J, Molloy R, Moss GW, Howe JR, Hughes TE. 1995. *The jellyfish green fluorescent protein: a new tool for studying ion channel expression and function*. Neuron 14:211-15.
Marshall RD. 1972. *Glycoproteins*. Annu Rev Biochem. 41:673-702.
Masters CL, Gajdusek DC, Gibbs CJ. 1981. *Creutzfeldt-Jakob disease virus isolations from the Gerstmann-Straussler syndrome with an analysis of the various forms of amyloid plaque deposition in the virus-induced spongiform encephalopathies*. Brain 104:559-88.
Matsunaga, Y, Peretz D, Williamson A, Burton D, Mehlhorn I, et. al. 2001. *Cryptic epitopes in N-terminally truncated prion protein are exposed in the full length molecule: dependence of conformation on pH*. Proteins 44:110-18.
McCutcheon S, Langeveld JPM, Tan BC, Gill AC, de Wolf C, et. al. 2014. *Prion protein-specific antibodies that detect multiple TSE agents with high sensitivity*. PLoS One 9:e91143.
McGowan J, Scott J. 1922. *Scrapie in sheep*. Scottish J.Agric. 5:365-75.
McKenzie D, Bartz JC, Marsh RF. 1996. *Transmissible mink encephalopathy*. Seminars in Virology 7:201-06.
Meyer RK, McKinley MP, Bowman KA, Braunfeld MB, Barry RA, Prusiner SB. 1986. *Separation and properties of cellular and scrapie priori protein*. Proc. Natl. Acad. Sci. USA 83:2310-14.
Meyer N, Rosenbaum V, Schmidt B, Gilles K, Mirenda, C, et. al. 1991. *Search for a putative scrapie genome in purified prion fractions reveals a paucity of nucleic acids*. J. Gen. Virol. 72:37-49.

Mitra, N, Shinha S, Ramya TN, Surolia A. 2006. *N-linked oligosaccharides as outfitters for glycoprotein folding, form and function*. Trends Biochem. Sci. 31:156-63.
Neuendorf E, Weber A, Saalmueller A, Schatzl H, Reidenberg K, et. al. 2004. *Glycosylation deficiency at either one of the two glycan attachment sites of cellular prion protein preserves susceptibility to bovine spongiform encephalopathy and scrapie infections*. J. Biol. Chem. 279:53306-16.
Oesch B, Groth DF, Prusiner SB, Weissmann C. 1988. *Search for a scrapie-specific nucleic acid: A progress report*. Ciba Found. Symp. 135:209-23.
Oesch B, Westaway D, Walchli M, McKinley MP, Kent SBH, et. al. 1985. *A cellular gene encodes scrapie PrP 27-30 protein*. Cell 40:735-46.
Palmer MS, Dryden AJ, Hughes JT, Collinge J. 1991. *Homozygous prion protein genotype predisposes to sporadic Creutzfeldt-Jakob disease*. Nature 352:340-42.
Pan KM, Baldwin MA, Nguyen J, Gasset M, Serban A, et. al. 1993. *Conversion of α-helices into β-sheets features in the formation of the scrapie prion proteins*. Proc. Natl. Acad. Sci. USA 90:10962-66.
Pattison IH, Millson GC. 1961a. *Further experimental observations on scrapie*. J. Comp. Path. Therap. 71:350-59.
Pattison IH, Millson GC. 1961b. *Scrapie produced experimentally in goats with special reference to the clinical syndrome*. J. Comp. Path. Therap. 71:101-08.
Pattison I. 1965. *Resistance of the scrapie agent to formalin*. J. Comp. Path. 75:159–64.
Pawel P. 2004. *Neuropathology of transmissible spongiform encephalopathies (prion diseases)*. Folia Neuropathologica 42:39-58.
Petersen RB, Parchi P, Richardson SL, Urig CB, Gambetti P. 1996. *Effect of the D178N mutation and the codon 129 polymorphism on the metabolism of the prion protein*. J. Biol. Chem. 271:12661-68.
Prusiner SB. 1982. *Novel proteinaceous infectious particles cause scrapie*. Science 216:136-44.
Prusiner SB, Scott M, Foster D, Pan KM, Groth D, et. al. 1990. *Transgenetic studies implicate interactions between homologous PrP isoforms in scrapie prion replication*. Cell 63:673-86.
Prusiner SB. 1991. *Molecular biology of prion diseases*. Science 252:1515-22.
Reik R, Hornemann S, Wider G, Billeter M, Glockshuber R, Wuthrich K. 1996. *NMR structure of the mouse prion protein domain PrP (121-231)*. Nature 382:180-82.
Rizzuto R, Brini M, Pizzo P, Murgia M, Pozzan T. 1995. *Chimeric green fluorescent protein as a tool for visualizing subcellular organelles in living cells*. Curr. Biol. 5:635-42.
Rogers M, Taraboulos A, Scott M, Groth D, Prusiner SB. 1990. *Intracellular accumulation of the cellular prion protein after mutagenesis of its Asn-linked glycosylation sites*. Glycobiology 1:101-09.
Sankaranarayanan S, De Angelis D, Rothman JE, Ryan TA. 2000. *The use of pHluorins for optical measurements of presynaptic activity*. Biophys. J. 79:2199-2208.
Sigurdson CJ, Manco G, Schwarz P, Liberski P, Hoover E, Hornemann S. 2006. *Strain fidelity of chronic wasting disease upon murine adaptation*. J. Virol. 80:12303-11.
Sigurdsson B. 1954. *RIDA, A chronic encephalitis of sheep with general remarks on infections which develop slowly and some of their special characteristics*. British Vet. J. 110:341-54.

Soto C. 2007. *Prions: The new biology of proteins*. Emerg. Infect. Dis. 13:959.
Spraker TR, Miller MW, Williams ES, Getzy DM, Adrian WJ, et. al. 1997. *Spongiform encephalopathy in free-ranging mule deer (Odocoileus hemionus), white-tailed deer (Odocoileus virginianus) and Rocky Mountain elk (Cervus elaphus nelsoni) in northcentral Colorado*. J. Wildl. Dis. 33:1-6.
Stahl, N, Borchelt DR, Hsiao K, Prusiner SB. 1987. *Scrapie prion protein contains a phosphatidylinositol glycolipid*. Cell 51:229-40.
Stahl N, Baldwin MA, Teplow DB, Hood L, Gibson BW, et. al. 1993. *Structural studies of the scrapie prion protein using mass spectrometry and amino acid sequencing.* Biochem. 32:1991-2002.
Telling GC, Scott M, Mastrianni J, Gabizon R, Torchia M, et al. 1995. *Prion propagation in mice expressing human and chimeric PrP transgenes implicates the interaction of cellular PrP with another protein*. Cell 83:79-90.
Thermo Fisher Scientific. *260/280 and 260/230 ratios*. (2009). [PDF File]. Retrieved from: http://www.nhm.ac.uk/content/dam/nhmwww/our-science/dpts-facilities-staff/Coreresearchlabs/nanodrop.pdf.
Tuzi NL, Cancellotti E, Baybutt H, Blackford L, Bradford B, et. al. 2008. *Host PrP glycosylation: a major factor determining the outcome of prion infection*. PLoS Biol. 6:e100.
Vilette D, Andreoletti O, Archer F, Madelaine MF, Vilotte JL, et. al. 2001. *Ex vivo propagation of infectious sheep scrapie agent in heterologous epithelial cells expressing ovine prion protein*. Proc. Natl. Acad. Sci. USA 98:4055-59.
Viles JH, Cohen FE, Prusiner SB, Goodin DB, Wright PE, Dyson HJ. 1999. *Copper binding to the prion protein: structural implications of four identical cooperative binding sites*. Proc. Natl. Acad. Sci. USA 96:2042-47.
Wells GAH, Scott AC, Johnson CT, Gunning RF, Hancock RD, et. al. 1987. *A novel progressive spongiform encephalopathy in cattle*. Vet. Rec. 31:419-20.
Westergard L, Christensen HM, Harris DA. 2007. *The cellular prion protein (PrP©)): Its physiological function and role in disease*. Biochim. Biophys. Acta. 1772:629-44.
Wildegger G, Liemann S, Glockshuber R. 1999*. Extremely rapid folding of the C-terminal domain of the prion protein without kinetic intermediates*. Nat. Struct. Biol. 6:550-53.
Wilesmith JW, Wells GA, Cranwell MP, Ryan JB. 1988. *Bovine spongiform encephalopathy: Epidemiological studies*. Vet. Rec.123:638-44.
Williams ES, Young S. 1980. *Chronic wasting disease of captive mule deer: A spongiform encephalopathy*. J. Wildl. Dis. 16:89-96.
Winklhofer KF, Heller U, Reintjes A, Tatzelt, J. 2003. *Inhibition of complex glycosylation increases the formation of PrPsc*. Traffic 4:313-22.
Wyatt JM, Pearson GR, Smerdon TN, Gruffydd-Jones TJ, Wells GAH, Wilesmith JW. 1991. *Naturally occurring scrapie-like spongiform encephalopathy in five domestic cats*. Vet. Rec. 129:233-36.